EFFECT OF DOLOMITE ON STRENGTH, RHEOLOGY AND MICROSTRUCTURE OF TERNARY BLENDED CEMENT

CLEAH MINAYO MASOLIA

A Thesis Submitted in Partial Fulfillment of the Requirements for Conferment of the Degree of Master of Science in Chemistry of Meru University of Science and Technology

2025

DECLARATION

This thesis is my original work and has not been presented for the award of a degree in any other institution.

SC406/201524/21

Signature……Date……...

Cleah Minayo Masolia

DECLARATION BY SUPERVISORS

This thesis has been submitted with our approval as University Supervisors

Signature……Date……...

Dr. Joseph Mwiti Marangu, Ph.D

Meru University of Science and Technology, Kenya

Signature……Date……...

Dr. Cyprian Muturia M'Thiruaine, Ph.D

Meru University of Science and Technology, Kenya

ACKNOWLEDGMENTS

I want to thank the Almighty God from the bottom of my heart for giving me the willpower and endurance to do this work. I sincerely thank Dr. Joseph Mwiti Marangu for all of his help and support during my academic career. Under his guidance, I have gained a great deal of knowledge and no words describe my gratitude. I am also grateful to Dr. Cyprian Muturia, my second supervisor, for his unwavering availability to provide guidance, insight, and support whenever needed. I will always be thankful to you for your assistance, which has helped me overcome many obstacles. I appreciate Prof. Luca Valentini's assistance. Mr. Victor Mutai Kiptoo is also acknowledged for his guidance throughout the research.

I want to acknowledge the Erasmus + KA107 Exchange Program for offering me a chance to undertake my research at the University of Padova in Italy. I also thank Meru University of Science and Technology for supporting me in this.

In conclusion, I express my gratitude to the material testing and research division for providing me with the opportunity to partially carry out my study at their establishments.

DEDICATION

This work is dedicated to my siblings Wicklife, Hilary, Titus, Sheila, and Silvia for their support and encouragement throughout the research. I further dedicate this work to my beloved daughter Nancy. Special thanks to Patrick for always being there for me. God's abundance favor be upon you.

TABLE OF CONTENTS

LIST OF FIGURES

LIST OF TABLES

LIST OF APPENDICES

ABBREVIATIONS

CH	Calcium Hydroxide
CHA	Coconut Husk Ash
DBG	Dolomite-Bauxite-Gypsum
DYS	Dynamic Yield Stress
FA	Fly Ash
ITZ	Interfacial Transition Zones
GGBS	Granulated Blast Furnace Slag
LC^3	Limestone Calcined Clay Cement
LBD	Light Burnt Dolomite
MPC	Magnesium Phosphate Cement
NMK	Nano-Metakaolin
OHA	Oat Husk Ash
OPC	Ordinary Portland cement
PDC	Portland Dolomite Cement
PPC	Portland Pozzolana Cement
RHA	Rice Husk Ash
SEM	Scanning Electron Microscopy
SMCs	Supplementary Cementitious Materials
SYS	Static Yield Stress
WTPS	Water Treatment Plant Sludge
XRD	X-Ray Diffraction
XRF	X-Ray Fluorescence

ABSTRACT

Supplementary cementitious materials (SCMs) have long been used in cement production to partially replace clinker, reducing CO_2 emissions and production costs while enhancing sustainability. Materials such as fly ash, silica fume and slag have been widely incorporated into cement formulations, improving performance and durability. However, the availability of these SCMs is diminishing due to declining industrial by-products prompting the search for alternative sources. A promising approach is the use of abundant calcined clay combined with limestone, forming a blended system known as Limestone Calcined Clay Cement (LC^3). This technology has gained attention as a viable solution to clinker reduction, offering comparable performance while utilizing widely available raw materials. In Africa, particularly in Kenya, the adoption of LC^3 technology faces a major challenge: the absence of high-quality limestone. Unlike regions with abundant pure limestone, many African countries primarily have low-grade limestone deposits, including dolomite. Inadequate high-quality limestone sources means that large-scale implementation would necessitate importing it, potentially increasing costs and limiting feasibility. Additionally, the low-quality limestone (dolomite) cannot be used in clinker production since its magnesium carbonate decompose to magnesium oxide that is associated with soundness during hydration. An alternative approach is to explore the use of locally available dolomite when it is not calcined to make a blended cement. In this study, the potential of incorporating dolomite in a ternary blended cement system alongside calcined clay was investigated. A replacement level of 45% was adopted, maintaining a dolomite-to-calcined clay ratio of 1:2. The study assessed the effect of combined clay and dolomite on cement strength, rheology and microstructure. The tested parameters were evaluated using compressive strength and rheometer machine, phase composition through X-ray Diffraction (XRD) analysis and Scanning Electron Microscopy (SEM) coupled with Energy Dispersive X-ray Spectroscopy (EDS). The pore was examined using Fiji, an open-source image analysis software program to refine the blends based on the SEM images. Compressive strength of 38 MPa after the 28th day was achieved relatively lower than OPC at 42.5MPa. Shear thinning property and low yield stress was obtained for the dolomitic blends indicating easy workability of the material. The results further showed a synergy between dolomite/limestone and calcined clay whereby additional phases formed on the 28th day including Hemicarboaluminate (Hc) and Monocarboaluminate (Mc). Higher pore refinement was observed with dolomite blends. The results showed that blending dolomite and calcined clay contributes significantly to mechanical properties in the same way as limestone and calcined clay. Microstructural analysis revealed a well-developed cement matrix with promising durability characteristics. These findings suggest that dolomite, when utilized serves as a viable alternative to high-purity limestone in ternary cement formulations, providing a sustainable and locally adaptable solution for clinker reduction in Africa. Dolomite is a suitable clinker substitute to clinker as it contributes to strength development of a ternary blended cement and also it has low yield stress thus enhanced workability.

CHAPTER ONE: INTRODUCTION

1.1 Background

Cement serves as a fundamental material used in the construction industries (Marangu, 2020; Zunino *et al.*, 2021). Its production is escalating annually to meet the increasing demand for social infrastructure and global housing needs (Gao *et al.*, 2015; Liu *et al*., 2021; Scrivener, 2014). According to Ngui *et al.* (2019) and Wachira *et al.* (2019), cement is widely used in a variety of projects such as bridges, block pavements, houses and dam construction. Over the past century, cement which is mostly used in concrete has helped produce over 5.30 billion m^3 of concrete yearly (Abbass et al., 2023).

Various types of cement are produced depending on their purpose. The common types of cement manufactured are Ordinary Portland Cement (OPC) and Portland Pozzolana Cement (PPC), with OPC historically dominating the market for several decades (Marangu, 2020). Research by Ige *et al*. (2022) underscores that cement industries emit approximately 8% of global anthropogenic Carbon (IV) Oxide (CO_2) during clinkerization. This process involves heating ground limestone, sand and clay in a kiln at temperatures around 1450° C (Gao *et al*.,2015) whereby limestone decomposes as shown in equation 1.1. Achieving these high temperatures typically involves burning coal and/or petroleum oil, releasing additional CO_2 into the atmosphere (Ngui *et al*., 2019; Wachira *et al*., 2019).

$$\mathrm{CaCO_3(s)} \xrightarrow[(1450^{o}\mathrm{C})]{\text{Heat}} \mathrm{CaO(s) + CO_2(g)} \qquad (1.1)$$

In developing nations, insufficient clinker production necessitates its importation a process further compounded by a tax of 25% on imported clinker in Kenya (Mutai *et al*., 2023). Consequently, the final product becomes prohibitively expensive. PPC produced in Kenya

incorporates volcanic ashes which are abundant in specific areas like Athi River, leading to the proliferation of cement industries in the region for easier access to raw materials (Marangu, 2020). Transportation of manufactured cement to other parts of the country exacerbates the price increase rendering cement unaffordable.

Since approximately 60% or more of the total materials used in construction is concrete, the housing crisis stems from the unaffordability of manufactured cement (Wachira *et al*., 2019). To manufacture affordable cement, the development of blended cement using supplementary materials has emerged as a promising method (Mutai *et al*., 2023a; Vaasudevaa *et al*., 2021). Blended cement has the potential to reduce the quantity of clinker used by about 50%. Sustainable interventions, such as blending limestone, calcined clay and OPC clinker commonly referred to as Limestone Calcined Clay Cement (LC^3), offer a viable approach to significantly reduce energy consumption and CO_2 emissions related to the manufacture of cement (Scrivener *et al*., 2018). This innovative blended cement is used in applications similar to OPC and PPC, with better durability and resistance to aggressive media attacks in presence of water. Additionally, limestone contributes to pore refinement enhancing the strength of cement. As highlighted by Scrivener *et al*. (2018), SCMs can be natural or waste materials but they are diminishing. Blending limestone and calcined clay (LC^2) offers the greatest potential for the continued use of SCMs as they diminish. An example of this is the worldwide availability of slag, which accounts for approximately 5% to 10% of the cement produced (Fantilli, 2021). Since the demand is increasing less rapidly than the demand for cement, Scrivener (2014) explains that slag availability in the coming century will decrease. The study done by Scrivener *et al*. (2018) further illustrates that iron production is in a limited number of countries. Fly ash available is only 30% of cement produced but its quantity and quality are

variable with less than one-third suitable for blending in cement (Fantilli, 2021). Moreover, limestone is in plenty but more than 10% alone in cement results in poor properties and more porous cement (Matschei *et al*., 2015).

Dolomite ($CaCO_3MgCO_3$) is abundantly available in Africa. 171 localities have been identified in East Africa (Di Salvo Barsi et al., 2020) with some localities in Kenya as shown in appendix iii. Dolomite can thus be used as an SCM in areas where pure limestone is not available and also reduce reliance on limestone since it's the main ingredient used for clinker production. Dolomite is a type of limestone that cannot be used to produce clinker because when it is burnt, it decomposes as shown in equation 1.2 to form magnesium oxide, calcium oxide, and carbon dioxide (Jiao *et al*., 2022; Rodriguez *et al*., 2012). Magnesium oxide hydrate slowly as shown in equation 1.3. to form brucite.

$$CaMg(CO_3)_2(s) \rightarrow CaO(s) + MgO(s) + CO_2(g) \quad (1.2)$$

$$MgO(s) + H_2O(l) \rightarrow Mg(OH)_2(aq) \quad (1.3)$$

This hydration process is accompanied by a volume expansion of about 118% which causes cracking of concrete or mortar (Rehsi, 2013). Dolomite can however be used in the production of blended cement as filler material and enhance the performance characteristics of the ternary blended cement, such as compressive strength, durability and resistance to various forms of deterioration like chloride and sulfates (Matschei *et al*., 2007). The utilization of raw dolomite, a form of limestone in cement production can be adapted to provide a solution to diminishing SCMs. According to Agrawal *et al*. (2021), approximately 4 – 5 billion tons of cement and 15 billion tons of crushed aggregates have been produced annually to manufacture 20 billion tons of concrete by incorporating dolomite. This study aimed to evaluate the performance of ternary blended cement incorporating dolomite by assessing key properties such as

compressive strength, rheological characteristics and microstructure development by contrasting it with LC^3.

1.2 Problem Statement

Cement production is a major contributor to anthropogenic CO_2 emissions, primarily due to the high-temperature calcination of limestone at 1450°C and the burning of fossil fuels to achieve this temperature. This process is highly energy-intensive, making clinker importation a necessity in many developing countries. In Kenya, for instance, clinker is imported at a compounded interest rate of 25%, significantly increasing the cost of cement and making it unaffordable for low- and middle-income households. As a result, the country faces a severe housing crisis, with an annual demand of 250,000 housing units, while the government can only provide 50,000. This shortage has led to a rise in homelessness and an increasing number of street children. With Kenya's rapidly growing population, the demand for affordable and decent housing continues to rise, necessitating a sustainable intervention to make cement production more cost-effective and environmentally friendly.

The construction industry is continuously exploring alternative and sustainable solutions to conventional cement production. One promising approach is the partial replacement of clinker with Supplementary Cementitious Materials (SCMs), which has been shown to reduce carbon emissions, lower costs, and enhance cement performance. However, some widely used SCMs, such as fly ash and slag, are becoming scarce, creating the need for new, locally available alternatives. Despite being abundant in Africa, dolomite remains underutilized as an SCM in cement production. Previous studies have explored the potential of dolomite in cement formulations, highlighting its ability to enhance strength development. However, the synergistic effect of dolomite with calcined clay in ternary blended cement has not been

comprehensively investigated. This study, therefore, seeks to examine the mechanical properties, rheological behavior, and microstructural development of cement containing dolomite and calcined clay. By incorporating locally available raw materials, this research aims to develop a cost-effective and sustainable cement blend, reducing reliance on imported clinker and contributing to the mitigation of CO_2 emissions. The findings of this study could provide a practical solution for Kenya and other developing nations, addressing the urgent need for affordable and environmentally friendly construction materials.

1.3 Significance of the Study

Cement production is a major contributor to global CO_2 emissions primarily due to the high-temperature calcination of limestone and the burning of fossil fuels. This poses a significant environmental challenge particularly in developing countries like Kenya, where the heavy reliance on imported clinker further escalates production costs. The high cost of cement directly impacts the affordability of housing contributing to a significant housing deficit. To address these challenges, sustainable and cost-effective alternatives to traditional cement production must be explored. Supplementary Cementitious Materials (SCMs) have been identified as a viable solution to partially replace clinker thereby reducing carbon emissions, energy consumption and production costs. However, commonly used SCMs, such as fly ash and slag are becoming scarce necessitating the need for alternative locally available materials. Dolomite and calcined clay are abundant in many parts of Africa but remain underutilized in cement production. Previous studies have shown that dolomite when used in cement blends can improve mechanical performance, yet its potential in ternary blended cement with calcined clay has not been fully explored. This study, therefore, seeked to bridge this knowledge gap by investigating the rheology, mechanical properties and microstructure of

dolomite-calcined clay blended cement. By utilizing locally available resources, this study aligned with global efforts toward sustainable cement production, reduced clinker dependence and contributed to affordable housing solutions in Kenya and beyond.

1.4 Research Objectives

1.4.1 General objective

To evaluate the effect of dolomite on the strength, rheology and microstructure of a ternary blended cement.

1.4.2 Specific objectives

i. To assess the physical and mechanical properties of prepared ternary blended cement.
ii. To determine the microstructure development of a ternary blended cement.
iii. To determine the rheology of the prepared ternary blended cement.

1.5 Research Questions

i. How do supplementary cementitious materials (SCMs) such as calcined clay, dolomite, and limestone influence the physical and mechanical properties of the cement blends?
ii. What relationships exist between microstructural features and the mechanical properties of the cement blends?
iii. How do the rheological properties of the prepared cement blends compare to those of OPC pastes?

CHAPTER TWO: LITERATURE REVIEW

2.1 Portland Cement Production and Composition

Cement is a hydraulic binder, that is a finely ground inorganic material which when mixed with water, forms a paste that sets and hardens through hydration reactions and processes and which once hardened stays stable and strong even in the presence of water (EAS 18-1 2017). According to Gao *et al*. (2015) for cement to be produced natural resources like limestone, sand and clay should be available. The production of cement consists of three main stages i.e., raw material preparation/quarrying, clinker production and cement processing. Raw material preparation involves quarrying and milling.

Compositions depend on the quality and properties of cement product demand. To produce clinker, the prepared raw materials are fed into the kiln and heated at a temperature of about 1450ºC (He *et al*., 2019; Sousa & Bogas, 2021). Finally, the produced clinker is blended with gypsum to make OPC or other mineral components e.g., slag and fly ash to make PPC (Sales *et al*., 2021).

2.1.1 Oxides composition of ordinary portland cement

Portland cement has an oxide composition that consists of major and minor oxides. The major oxides include calcium oxide, silicon oxide aluminium oxide and iron oxide while minor oxides include magnesium oxide (MgO), Sulfur Trioxide (SO_3), and alkali oxides (K_2O and Na_2O) (Kurdowski & Thiel, 2018). The approximate percentage of each oxide in Portland cement is shown in Table 2.1

Table 2.1

Oxide Composition in Portland Cement

Oxide Nomenclature	Chemical Nomenclature	Chemical Formula	Cement Notation	Composition by mass (%)
Calcium oxide	Lime	CaO	C	60 – 67
Silicon oxide	Silica	SiO_2	S	17 - 25
Aluminium oxide	Alumina	Al_2O_3	A	3-8
Iron oxide	Ferric Oxide	Fe_2O_3	F	3-9
Magnesium oxide	Magnesia	MgO	M	< 5
Sulfur Trioxide	Sulphuric hyrite	SO_3	S	< 3
Potassium oxide	Alkali Oxide	K_2O	K	< 1
Sodium Oxide	Alkali Oxide	Na_2O	N	<1

Source: (Selman & Ali, 2012; Abdunnabi, 2012).

CaO is a primary component of Portland cement. It is derived from limestone during the calcination process (Aïtcin, 2016). Appah (2021), reported that CaO is used as an expanding agent to overcome contraction as binder slurry sets. It can also be used to increase the thickening time of binder, from about 100 to 380 minutes, which is beneficial for the proper placement of cement especially in boreholes (Bediako & Amankwah, 2015). It can react with silica to form tri-calcium-silicate hydrate (alite) and di-calcium silicate hydrate (belite) in the hydration process which is essential for the cement's binding properties as shown in equations 2.1 and 2.2 respectively (Brown, 2020). It is the hydration reactions of these silicate phases that are primarily responsible for the development of concrete strength. However, both the

rates of reaction and the relative proportions of the hydration products formed are quite different. Compared to belite, alite hydrates substantially more quickly. According to Okoye (2017) SiO_2 reacts with CaO to form calcium-silicate hydrate during hydration.

$$3CaO + SiO_2 \rightarrow 3CaO{\cdot}SiO_2 \quad (2.1)$$

$$2CaO + SiO_2 \rightarrow 2CaO{\cdot}SiO_2 \quad (2.2)$$

When alumina and calcium oxide combine, calcium aluminate phases such as tricalcium aluminate (C_3A) and dicalcium aluminate (C_2A) are formed (Mutai *et al*., 2023). High alumina binder is used when early strength development is required; however, high alumina binder is unsuitable for large-scale concrete work (Khelifi *et al*., 2017). This is because it affects its sulfate resistance and heat evolution characteristics during the early stages of hydration, resulting in higher peak temperatures and faster heat liberation rates (Aïtcin, 2016; Qinfei *et al*., 2019).

Fe_2O_3 imparts color to the binder and influences its setting time and strength development (Zunino *et al.*, 2021). It participates in the formation of aluminoferrite phases, such as tetracalcium aluminoferrite (C_4AF), which contribute to the concrete's mechanical properties. Iron oxide also affects the binder's durability, particularly its resistance to sulfates and alkalis attacks (Ijaz *et al*., 2022).

MgO is made from unprocessed materials that comprise magnesium such as dolomite or magnesite (Zheng *et al.*, 2012). Magnesium oxide contributes to the overall composition and mechanical properties of binder material. Studies by Unluer and Al-Tabbaa (2015) reveal that replacing MgO with 50% brucite does not compromise the strength of the binder because the reaction of periclase with water to form brucite as shown in equation 2.3 does not significantly

increase volume of the hydrated paste. The results from the study show that MgO replacement by brucite achieved strength results between 13.2 –18.5 MPa on the 7th day.

$$MgO(s) + H_2O(l) \rightarrow Mg(OH)_2(s) \quad (2.3)$$

SO_3 is made from unprocessed materials that comprise sulfur, such as gypsum (calcium sulfate) or sulfate-bearing minerals. The presence of sulfur in raw materials like gypsum or sulfate-bearing minerals can lead to the release of sulfur dioxide (SO_2) during the binder manufacturing process according to reaction 2.4.

$$CaSO_4 \rightarrow CaO + SO_2 + \frac{1}{2}O_2 \quad (2.4)$$

Sulfur trioxide influences the setting time by controlling the flush setting as it can react with water and calcium oxide (CaO) during binder hydration to form calcium sulfate (equation 2.5). It reacts with calcium oxide during hydration to form calcium sulfate compounds, which can affect the binder's early and final setting times.

$$SO_3 + CaO + 2H_2O \rightarrow CaSO_4{\cdot}2H_2O \quad (2.5)$$

Sulfur trioxide reacts with calcium oxide (CaO) during cement hydration to form calcium sulfate compounds such as gypsum (calcium sulfate dihydrate, $CaSO_4{\cdot}2H_2O$) or ettringite (calcium sulfate aluminate hydrate, $Ca_6Al_2(SO_4)3(OH)_{12}{\cdot}26H_2O$) (Equation 2.6). These compounds can influence both the early and final setting times of binder material.

$$3CaO.Al_2O_3 + 3CaSO_4.2H_2O + 26H_2O \rightarrow Ca_6Al_2(SO_4)_3(OH)_4.26H_2O \quad (2.6)$$

Excessive sulfur trioxide content can lead to delayed setting and reduced early strength, while insufficient sulfur trioxide may result in inadequate sulfate resistance (Yamashita *et al*., 2020). Proper control of sulfur trioxide content is essential to ensure optimal cement performance in various environmental conditions.

Alkalis can accelerate the setting time of binder, particularly in the early stages of hydration. This acceleration occurs due to their role as alkali activators, which promote the dissolution of reactive silica and alumina in cementitious materials (Unluer & Al-Tabbaa, 2015). The presence of alkalis increases the rate of hydration reactions leading to the faster formation of CSH which is responsible for the binder's setting. As a result, the binder mixes containing greater than 2% alkalis tend to exhibit shorter setting times compared to those with lower alkali content. Excessive potassium oxide and sodium oxide content can potentially accelerate the setting time, leading to flash setting, where the cement paste rapidly transforms into a rigid mass within a very short period after mixing (Selman & Ali, 2012). Proper control and optimization of these oxides are necessary to achieve the desired cement performance. Equations for the reaction between alkalis and silica and then consumption of portlandite are as shown in equations 2.7 and 2.8 respectively

$$K_2O + SiO_2 + H_2O \rightarrow K_2SiO_3 + H_2O \quad (2.7)$$

$$K_2SiO_3 + Ca(OH)_2 + H_2O \rightarrow CaSiO_3.H_2O + 2KOH \quad (2.8)$$

Alkalis can also influence the early strength development of cement. By accelerating the hydration reactions, they promote the formation of hydration products at an earlier stage, resulting to rapid development of strength. Okoye, (2017) reported an increased alkali concentration (Na_2O/Al_2O_3=0.62) that resulted to highest compressive strength of 48.20 MPa.

2.1.2 Manufacture of Portland Cement

The raw materials used in producing Portland cement should be materials rich in silicon, calcium, aluminum, and iron oxides. These constituents undergo heating at temperatures ranging from approximately 1200^{o}C to 1450^{o}C. The process yields four principal cement components, as outlined in Table 2.2 (Zunino & Scrivener, 2021).

Table 2.2

Major Mineral Constituents of Portland Cement

Compound	Abbreviation	Chemical formula	Typical composition (%)
Tri-calcium silicate	C_3S	$3CaO.SiO_2$	60-70
Dicalcium silicate	C_2S	$2CaO.SiO_2$	10-20
Tricalcium aluminate	C_3A	$3CaO.Al_2O_3$	5-10
Tetracalcium aluminoferrite	C_4AF	$4CaO.Al_2O_3Fe_2O_3$	3-9

The blending and grinding of raw materials can be achieved via either the dry or wet method. In the wet process, a slurry is created in wash mills as raw materials are crushed and ground (Szostak & Golewski, 2021; Sales *et al*., 2021). This slurry typically contains 30–50% water content with the majority of particles being smaller than 90 μm. Following its formation the slurry is conveyed into a tank before being transferred to the upper section of the rotary kiln. As the slurry descends the kiln, it is progressively exposed to high temperatures. However, this method is energy-intensive leading many manufacturing firms to transition away from it (Kurdowski, 2014).

In the dry process, raw materials crunch until they attain particle sizes lower than 90 μm. This process maintains controlled proportions of materials fed into the grinding mill. Subsequently, the resulting dry powder is transferred to a blending silo for final adjustments to achieve the desired cement proportions. Within the silos, upward movement is induced by compressed

air. At this stage, the raw materials typically contain around 0.2% moisture. Following this they are sent via a pre-heater where the ascending gases from the kiln suspend the particles (Kapustin & Bashkatov, 2020; Salas *et al*., 2016).

2.2 Hydration of Portland Cement

Cement gains strength when it comes into contact with water. This process is known as hydration of cement and it involves heat generation. The clinker phases shown in Table 2.2 hydrate when the binder is mixed with water to form hydrated products. C_3S is the primary phase responsible for the early strength development and heat generation during cement hydration (Yamashita *et al*., 2020). It forms calcium silicate hydrate quickly when in contact with water to form calcium silicate hydrate (CSH) gel and calcium hydroxide (CH) as in equation 2.9 (Kurdowski, 2014). C_3S contributes significantly to the initial strength gain of concrete, making it essential for achieving early-age strength (Scrivener *et al*., 2018).

$$2C_3S + 6H \rightarrow C_3S_2H_3 + 3CH \quad (2.9)$$

C_2S hydrates more slowly than C_3S but still helps concrete gain strength over time (Mutai *et al.*, 2023). It reacts with water to form CSH gel and CH, similar to C_3S. While C_2S hydration kinetics are slower compared to C_3S, it contributes to the long-term strength and durability of concrete (Cao *et al*., 2021). The hydration process of C_3S generates a lot of portlandite than that of C_2S because C_3S is richer in lime than C_2S (Aïtcin, 2016).

C_3A reacts rapidly with water and gypsum to form ettringite as in equation 2.10. Ettringite contributes to early strength development but can also lead to volume expansion and cracking if not properly controlled. Despite its rapid reactivity, excessive C_3A content can cause flash setting and reduce the workability of concrete. Proper control of C_3A is crucial for achieving desirable properties. This phase provides early strength and contributes to the cement's sulfate

resistance. However, excessive amounts of C_3A can lead to the risk of sulfate attack (Wang *et al.*, 2018).

$$C_3A + 3CaSO_4.2H_2O + 26H_2O \rightarrow Ca_6Al_2(SO_4)_3(H_2O)_{12}.26\,H_2O \quad (2.10)$$

(Ettringite)

C_4AF hydrates relatively slowly and contributes to the late-strength development of concrete (Aïtcin, 2016). It reacts with gypsum in the presence of water to form ettringite and a by-product of iron hydroxide as shown in equation 2.11. While C_4AF does not contribute significantly to early strength, it enhances the long-term strength and sulfate resistance of concrete (Dixit *et al*., 2021).

$$2C_4AF + 7H \rightarrow C_3(A,F)H_6 + 2Fe(OH)_3 \quad (2.11)$$

2.3 The Role of Supplementary Cementitious Materials (SCMs) in Cement Production

These are pozzolana materials that chemically react with lime (portlandite) produced during the hydration of cement (Cao *et al*., 2021; Zunino & Lopez, 2016). During the hydration of cement, tricalcium aluminate reacts with gypsum to form ettringite and heat while C_3S and C_2S to form CSH and lime as in equations 2.12, 2.13, and 2.14 respectively (Jansen *et al*., 2012). Equation 2.12 produces a lot of heat. CH formed in 2.13 and 2.14 is prone to attacks in an acidic medium.

$$C_3A + 3C\bar{S}H_2 + 26H \rightarrow C_6AS_3H_{32} \quad (2.12)$$

$$C_3S + 6H \rightarrow C_3S_2H_3 + 3CH \quad (2.13)$$

$$C_2S + 4H \rightarrow C_3S_2H_3 + CH \quad (2.14)$$

In the presence of a pozzolana, CH is consumed by silicate or silicatealumina forming calcium silicate hydrate which is an additional phase (Abdulqader *et al*., 2023; Zunino & Scrivener,

2021). Aluminium in SCMs combines with CH to form hemicarboaluminate and monocarboaluminate (Mutai *et al*., 2023).

Generally, SCMs may be artificial, industrial, or agricultural (Scrivener *et al*., 2018). In research conducted by Hwang *et al*. (2016), mixtures of cement and ash from rice husks were made. Rice Husk Ash mix was prepared (M_1 10% PC: 0% RHA, M_2 7.5% PC: 2.5% RHA and M_3 5% PC: 5% RHA) and tested. According to the findings, compressive strength decreased when RHA increased. Naturally occurring SCMs like clay which is calcined and then blended with clinker and limestone to produce LC^3 have been studied too. Study by (Scrivener *et al*. (2018) found out that kaolinite content of ≥ 40% produces effective results when blended with limestone to produce LC^3. LC^3 has a reduced amount of clinker to about 40-50% with 30% - 40% calcined clay, 15% limestone and 5% gypsum (Scrivener *et al*., 2018).

SCMs such as fly ash, slag, silica fume, and metakaolin are commonly used as clinker substitutes. Fly ash is a by-product of coal combustion in power plants and is widely used due to its pozzolanic properties. Ground Granulated Blast Furnace Slag (GGBFS), obtained from iron production, is another popular SCM renowned for having a strong reaction and ability to improve concrete durability. Silica fume, a byproduct of silicon metal and ferrosilicon alloy production, is valued for its high pozzolanic activity and ability to enhance early-age strength development. Metakaolin, produced by calcining kaolin clay, is used because of its high reactivity and ability to improve cement performance in various applications (Mehta & Monteiro, 2014).

Studies by Zhang *et al*. (2017) and Thomas *et al*. (2020) demonstrate the effectiveness of GGBFS in enhancing the robustness and mechanical characteristics of concrete. Their

research reveals that GGBFS contributes to increased compressive and flexural strengths, reduced permeability and enhanced resistance to chloride penetration and sulfate attack. Research by Malhotra and Mehta (2012) suggests using fly ash in combination with limestone in concrete mixes improves workability, reduces heat of hydration and enhances long-term strength and durability. They found that fly ash reacted with CH to produce additional CSH gel, resulting in denser microstructures and reduced permeability. Another study by Thomas *et al*. (2013) investigated the influence of fly ash on the sulfate resistance of concrete. They found that fly ash mitigates sulfate attack by reducing the availability of CH and forming ettringite, which helps to seal microcracks and inhibit sulfate ingress.

2.4 Carbonate Rocks

Carbonate rocks are a class of sedimentary rocks composed primarily of carbonate minerals. The two most common carbonate minerals found in these rocks are calcite (calcium carbonate, $CaCO_3$) and dolomite (calcium magnesium carbonate, $CaMg(CO_3)_2$) (Hartmann & Moosdorf, 2012; Sharma *et al*., 2021). Calcite is composed of tiny fossils, shell fragments, and other fossilized debris (Wang *et al.,* 2018). It exists in two types i.e. calcite limestone and dolomitic limestone (Taylor *et al*., 2017), which have a composition of calcium carbonate ($CaCO_3$) and calcium carbonate magnesium carbonate ($CaMg(CO_3)_2$) respectively. Additionally, calcite may occur in sedimentary, metamorphic, or igneous rock formations.

Calcite deposits are widespread globally, occurring in various geological formations such as marine sedimentary rocks, limestone caves, and fossilized coral reefs (Ngcofe & Cole, 2014). The chemical composition of calcite primarily comprises calcium carbonate, typically ranging from 70% to 95%, with minor impurities such as clay, silica, organic matter and iron oxide (Mehta and Monteiro, 2016). The purity and chemical composition of calcite deposits varies

significantly depending on geological factors, with higher-purity calcite typically preferred for cement production due to its chemical reactivity of calcium oxide formed after calcination. Calcites have been classified based on the geology, grain size microstructure, texture, and principal impurities, without forgetting industrial use. Limestone can be ultra-high calcium limestone (more than 97.5% $CaCO_3$) and high calcium limestone (95 - 97.5% $CaCO_3$). High-purity carbonate rocks are more than 95% and it comprised of calcium carbonate and magnesium carbonate. High-magnesium dolomite has more than 43% magnesium carbonate. Calcite plays a critical role in cement production as a primary raw material used in the manufacturing process. During this process, calcite is burnt at high temperatures and decomposes to form calcium oxide (Lime) and carbon dioxide (equation 2.15). Pure calcite is used because during the decomposition process, it loses 44% of its weight (Cantonati *et al*., 2016). The lime reacts with raw materials that are fed into the kiln which are rich in oxides of silicon, calcium, aluminum, and iron to form the clinker phases (Mutai *et al.*, 2023). These clinker phases are responsible for imparting strength and durability to the cementitious matrix.

$$CaCO_3(s) \xrightarrow[1450^oC]{\text{Heat}} CaO(s) + CO_2(g) \quad (2.15)$$

Gypsum is added to cement which helps to regulate the setting time and rheological properties of cementitious pastes, influencing workability and ease of placement during concrete construction.

Despite the widespread use and significant contributions of calcite to cement production, it still presents several limitations and challenges that warrant consideration. One notable limitation is the presence of impurities and contaminants in calcite deposits, such as clay, silica and organic matter, which can adversely affect the binder's mechanical properties (Mehta and Monteiro, 2016). High levels of impurities may lead to increased energy

consumption, kiln ring formation, and variability in clinker composition, resulting in reduced cement robustness and longevity (Ngcofe & Cole, 2014).

The accessibility and availability of high-quality calcite deposits may pose challenges, particularly in regions with limited geological resources or environmental constraints (Taylor *et al.,* 2017). Environmental concerns associated with calcite quarrying, such as habitat destruction, land degradation, and groundwater contamination, require attention to guarantee sustainable limestone extraction practices (Mehta and Monteiro, 2016). Moreover, the use of calcite while making cement is subject to regulatory standards and specifications governing cement quality, chemical composition, and effects on the environment (Taylor *et al.*, 2017). To adhere to these requirements, careful monitoring and control of limestone sourcing, processing, and utilization throughout the cement manufacturing process.

2.4.1 Dolomite

Dolomite is a double carbonate mineral containing both calcium and magnesium in a 1:1 molar ratio. It is a type of limestone that has a chemical formula of ($CaMg(CO_3)_2$). It has been used as an aggregate for concrete manufacturing as well as a partial substitute for Portland cement (Agrawal *et al*., 2021). This is a reactive cementitious material that is added to cement to increase its strength (Zajac *et al*., 2014). The dolomitization reaction takes place when portlandite reacts with dolomite according to equation 2.16. This reaction is unfavored by high temperatures and alkalinity content (dedolomitization).

$$CaMg(CO_3)_2 + Ca(OH)_2 \rightarrow 2CaCO_3 + Mg(OH)_2 \quad (2.16)$$

Dolomite being an SCM has additional carbonate ions for alumina to bind with (Matschei *et al*., 2015; Zajac *et al*., 2014). Although brucite (magnesium hydroxide) makes binder unsound, research reveals that the above reaction cannot lead to expansion because it is

accompanied by reduced solid volume as in equations 2.17 a and b. This reaction involves the formation of calcium hydroxide and magnesium silicate. Both of these products are typically solid, so they occupy space. The formation of new solid phases can lead to a reduction in overall volume due to differences in crystal structure or packing efficiency (Kuenzel *et al*., 2018). It can fill the spaces which results in a well pore-filled structure leading to improvement in the durability and performance of blended cement.

a) $Mg(OH)_2 + 2H_2O \rightarrow Mg(OH)_2.2H_2O$ (2.17)

b) $Mg(OH)_2.2H_2O + CaSiO_3 \rightarrow Ca(OH)_2 + MgSiO_3$

2.4.2 Incorporation of dolomite in portland cement

Light-burnt dolomite (LBD) has been incorporated in cement as a replacement for clinker by Chen *et al*. (2021) and results show that incorporating 10% LBD, particularly calcined at 800°C for 2.0 hours, significantly enhances the compressive strengths of blended cement. This can be attributed to microstructural changes resulting from the filler effect and the hydration reactivity of dolomite. An interesting observation made from the same study is water requirement for achieving normal consistency of blended cement increases as dosage increases. Investigations by Mikhailova *et al*. (2013) confirmed that finely ground dolomite can be used as cementitious material to produce binder. Incorporating more 25% dolomite into cement reduces compressive strengths after 14 and 28 days (Jiao *et al*., 2022). This is because C_3S and C_2S phases are reduced and less reactive phases are formed as shown in equation 2.18. Utilization of dolomite is an effective way that leads to dense microstructure (Xu *et al*., 2021).

$CaO{\cdot}SiO_2{\cdot}H_2O + CaMg(CO_3)_2 \rightarrow CaO{\cdot}SiO_2{\cdot}H_2O + CaMg(CO_3)_2 + Ca(OH)_2$ (2.18)

Dolomite has been used together with Magnesium phosphate to form Magnesium Phosphate Cement (MPC) formulations by chemically combining Dolomite Bauxite Gypsum (DBG) powders, leading to the production of MPC containing ye'elimite as in equation 2.19. The investigation revealed that MPC pastes incorporating calcined DBG powders exhibited favorable properties, including high early compressive strength and good volume stability (Agrawal *et al*., 2021; Salvo *et al*., 2020). Furthermore, the participation of ye'elimite in hydration reactions was observed, contributing to the development of hydration products and enhancing the water resistance of MPC pastes equation 2.20. The emergence of new amorphous hydration products during water curing also suggested potential benefits for the compressive strength development of MPC pastes. Overall, these findings highlight the potential of dolomite usage to improve the performance and properties of the resulting cementitious materials. Another use of dolomite is it has been utilized to investigate the mechanical and durability properties of concrete containing dolomite as coarse aggregate (Agrawal *et al*., 2021; Mikhailova *et al*., 2014a). The findings reveal that addition of 20% wt of dolomite contributes to increased strength from 7^{th} day up to later age by acting as a pore filler thus increasing the durability and strength of concrete. The use of dolomite to replace clinker in cement leads to reduction in setting time because the presence of magnesium in dolomite alter the hydration chemistry and lead to faster setting (Machner *et al.,* 2017). Salvo *et al*. (2020) illustrates that this is attributed to the stimulation of Portland cement hydration caused by the nucleation and the short interparticle distance due to the incorporation of finely divided particles of the filler material. These findings are similar to Warren (2020) who reported that when dolomite is incorporated as an aggregate in concrete, it contributes to improved mechanical properties.

$$4CaO.Al_2O_3 + 2CaSO_4 \rightarrow Ca_4Al_6O_{12}SO_4 \quad (2.19)$$

$$Al_6O_{12}SO_4 + 26H_2O \rightarrow CaO.2SO_3.Al_2O_3.15H_2O + 4\,Ca(OH)_2 \quad (2.20)$$

Study conducted by Bentz & Ferraris (2018) have highlighted a significant impact of incorporating dolomite into cementitious blends on the rheology and properties of fresh concrete. Specifically, Bentz *et al.* (2017) observed that using dolomite powder in concrete influences the flowability and workability of concrete, with dosages of more than 25% resulting in a reduction of viscosity and yield stress. Additionally, Bentz & Ferraris (2018) reported that coarse dolomite powder can effectively alter the viscosity and segregation resistance of self-compacting concrete mixes. These findings underscore the importance of considering dolomite as a potential rheology-modifying agent in concrete mix design, but this can be reduced by using an admixture to improve the flowability of cement, without compromising strength.

2.5 Composition of Limestone Calcined Clay Cement (LC^3)

Limestone Calcined Clay Cement (LC^3) is a ternary binder that consists of clinker, clay which is calcined, limestone and gypsum which is mixed to make a composite binder (Scrivener, 2014). Supplementary cementitious materials which are capable of reducing the clinker content have also been used in the manufacture of blended cement. When kaolinite clay is heated at about 600 – 800 ^{0}C, it produces a reactive amorphous phase capable of reacting with portlandite, to form the second binder as shown in Equation 2.21 (He *et al*., 2019; Mutai *et al*., 2023; Tambara Júnior *et al*., 2023). LC^3 produced is affordable as it is a blend of SCMs with 50% clinker(Zunino et al., 2021). The level of carbon dioxide produced is also reduced. The general composition of LC^3 is shown in Figure 2.1.

$$2Al_2Si_2O_7 + 3Ca(OH)_2 + 10H_2O \rightarrow 3CaO.Al_2O_3.3CaSiO_5.32H_2O \quad (2.21)$$

Figure 2.1

Mixing proportions of the LC^3 blend

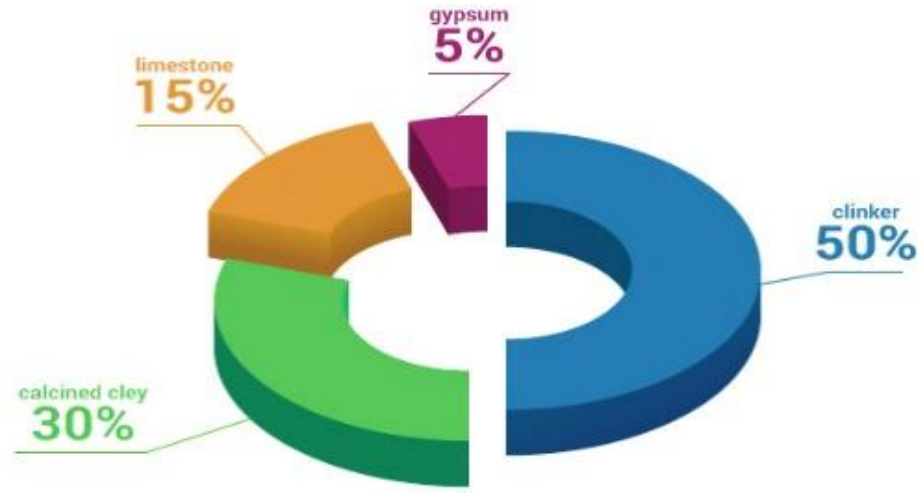

According to Dhandapani *et al.* (2018), LC^3 can be prepared with low-calcite limestone that contains impurities such as magnesium carbonate and quartz and from their findings, they found that LC^3 surpassed OPC in terms of mechanical properties at all curing ages up to one year. Similar studies have been done by Scrivener *et al*. (2018); Zunino *et al*. (2021) and reported that blended cement exhibited a higher of 34.4 Mpa for LC^3 than OPC having 32.1 Mpa on the 28th curing day. This is attributed to the properties of limestone and calcined clay, which improve the particle packing of the cementitious system. The fine particles of limestone fill in the voids between larger particles, resulting in a denser and more compact matrix.

LC^3 technology has gained traction globally as a promising alternative to OPC. Ongoing research and development efforts focus on: optimizing LC^3 formulations, refining production processes and evaluating performance in various applications to facilitate widespread adoption and implementation in the construction industry (Scrivener, 2 014).

In the quest to optimize LC^3 formulations, exploration of a range of strategies is in place like careful selection of raw materials such as limestone and kaolinite clay, evaluating their chemical composition, mineralogy, and reactivity to achieve desired properties while minimizing costs and environmental impact (Zunino & Scrivener, 2021b). Experimentation with blending ratios of limestone, and calcined clay helps determine the optimal proportions for enhancing strength, durability, workability, and setting time. Additionally, Scrivener *et al*. (2018) investigated the use of chemical additives, including pozzolans and mineral admixtures like the superplasticizer, to further enhance workability without compromising mechanical properties and sustainability. Advanced characterization methods such as X-ray diffraction and scanning electron microscopy (SEM) are used to study the microstructure and hydration products of LC^3 (Zunino *et al*., 2021).

Refining production processes is essential for improving the efficiency, sustainability, and quality of LC^3 cement. This involves advancements in calcination techniques for clay, including traditional rotary kiln calcination, flash calcination, or innovative approaches such as microwave or plasma-assisted calcination (Scrivener *et al.*, 2018). Optimization of grinding and blending processes ensures the production of finely ground calcined clay with a uniform distribution of ingredients (Zunino *et al.,* 2021). Engineers design and operate cement kilns to maximize thermal efficiency, minimize emissions, and ensure consistent production of high-quality binders *(Salas et al.*, 2016). Strict quality control procedures are put in place throughout the production process to monitor chemical composition, fineness, and performance, ensuring compliance with specifications and standards (Jiao *et al*., 2022).

The evaluation of LC^3 performance in various applications is essential for determining its appropriateness and potential benefits. Comprehensive laboratory testing assesses

performance properties like flexural strength, shrinkage, compressive strength, permeability, and resistance to chloride and sulfate attacks (Marangu, 2020; Zunino & Scrivener, 2021a). Long-term durability studies simulate real-world conditions to assess resistance to factors such as chemical exposure, carbonation, and abrasion, predicting the service life of structures built with LC^3 cement (Abdulqader *et al.*, 2023; Ijaz *et al.*, 2024).

2.6. Strength Development of Hydrated Cement

Strength is a crucial parameter that is used to determine if the material used meets the standards required (Tao *et al.*, 2022). In Kenya, the method employed to test this parameter is illustrated in KS EAS 148-1: 2017. The standard specifies different classes of OPC and PPC with varying strengths. Additionally, it also outlines various other parameters including fineness, setting time and chemical composition and soundness that cement must conform to meet the specified quality criteria. According to Marangu (2020), strength increases as the curing period increase. As per the findings from the study, OPC showed a greater compressive strength compared to LC^3 and PPC at all the curing ages from 2 - 28 days. This can be linked to the differences in the relative amount of C_3S and C_2S between the blended cements and OPC.

SCMs that are often utilized include: fly ash, slag and silica fume which enhance performance and sustainability of concrete. Research by Mehta and Monteiro (2014) highlights the role of SCMs in improving the long-term strength development of cement through various mechanisms, including filler effect, pozzolanic reaction and nucleation of hydration products. SCMs act as fine particles that fill the voids between cement grains, leading to denser concrete microstructures (Olawuyi & Olusola, 2010). This densification improves the packing of cementitious materials, thereby enhancing the strength and reducing permeability (Machner

et al., 2017). Extra calcium silicate hydrate (CSH) gel is created when SCMs such fly ash and slag react with the calcium hydroxide (CH) formed during cement hydration. This pozzolanic reaction contributes to the formation of secondary hydration products resulting in increased strength and reduction in permeability (Mehta & Monteiro, 2014).

Curing conditions plays a vital part in the strength development of cementitious materials. According to Kurdowski (2020), adequate moisture and temperature during curing are essential for the hydration process to proceed optimally, leading to the development of high strength. Proper curing conditions provide the necessary environment for hydration to occur efficiently. Adequate moisture ensures continuous hydration reactions, resulting to the formation of products such as calcium silicate hydrate (CSH) gel, which contribute to strength development (Scrivener *et al*., 2018). The duration of curing significantly influences the final strength of concrete. While early-age strength development occurs rapidly, long-term strength continues to increase over time with proper curing. Extending the curing period allows for more complete hydration and contributes to higher ultimate strength (Dhandapani *et al.,* 2018; Zunino & Scrivener, 2021).

2.7 Microstructure Development of Hydrated Cement

The microstructure of a hydrated cement can be investigated by either preparing a sample for XRD to determine peaks formed or by using a Scanning Electron Microscope (SEM) (Sharma *et al.,* 2021). Mikhailova *et al*. (2014) examined how the addition of dolomite affected the compressive strength of concrete and discovered that the microstructure of concrete without fine limestone powder had a porous, open-grain structure dominated by macropores. Dolomite addition results in an increase in the number of centers which initiates more intensive crystallization that in turn results in an increase in hydration rate. They found in their research

that dolomite ultrafine particles act as additional crystallization grains, and the optimal content of dolomite is 25% of cement weight since at this amount fine concrete has the highest strength and is non-porous.

SEM obtains a high-resolution imaging of the microstructure of hydrated cement paste. By examining the surface morphology and pore structure at the microscale, SEM analysis provides information on the distribution of hydration products, porosity and Interfacial Transition Zones (ITZ) between cementitious phases and aggregates (Kurdowski, 2019). SEM images reveal the morphology of CSH gel, unhydrated cement particles and voids. Qinfei *et al*. (2019a) illustrate that needle-like Aft phases are observed in the clinker paste, limestone and metakaolin and some unreacted metakaolin, which was in agreement with the XRD results on the third day. On the 28^{th} day, the LC^3 system showed more holes and cracks, which means it has a relatively loose microstructure. Similar results by (Jiang *et al*., 2020) show that the major hydration products involve CSH gels and small needle-like ettringite which was in agreement with the XRD results.

The pore structure and porosity of hydrated cement paste are important elements influencing its mechanical and transport properties. High porosity and interconnected pore networks can lead to reduced strength, increased permeability, and susceptibility to deleterious processes such as freeze-thaw damage and chemical ingress (Scrivener & Snellings, 2018). Understanding the distribution and characteristics of cement matrix pores is essential for predicting performance and durability. This can be done through the analysis of hydrated cement paste. Increased porosity compromises the packing density of cementitious materials, resulting in reduced mechanical strength (Zunino & Scrivener, 2021). The presence of large voids and interconnected pores creates discontinuities in the paste matrix, which weaken the

overall structure and diminish load-bearing capacity. Porous cement paste allows for easier ingress and movement of fluids, including water, gases, and aggressive chemicals. Elevated permeability enhances the susceptibility of concrete to moisture-related deterioration mechanisms such as corrosion of embedded reinforcement and alkali-silica reaction (Xu *et al*., 2022).

2.8 Rheological Properties for Cement Paste

Rheology is the study of the flow and deformation of matter (Athira & Bahurudeen, 2022). The study is responsible for explaining the relationship between force, deformation and time using various properties like flow curves, viscosity curves (shear thinning and thickening) and yield stress among others (Sales *et al*., 2021). The viscosity curves can also help identify whether shear thinning or shear thickening behavior of the material. Understanding the flow curve and viscosity curve of LC^3 enables engineers to optimize its rheological properties, ensuring proper workability, pumpability, and application in various construction processes (Chen *et al.*, 2023).

2.8.1 Rheological properties of blended cement - viscosity and flow behavior

Viscosity is a measure of a material's resistance to flow (Khayat & Mikanovic, 2014). It determines the thickness or fluidity of a material and is influenced by factors such as particle size, concentration, and interactions between particles. In the reference to clay-based cement, viscosity is the resistance of the cementitious mixture to flow (Sales *et al*., 2021). On the other hand, the flow behavior of clay-based cement describes how it behaves when subjected to external forces or stresses. It can vary depending on the concentration and arrangement of clay particles, the water content, and other factors. According to Ferreiro *et al*. (2017), the

viscosity and flow behavior of clay-based cement can vary depending on several factors such as clay content, water-to-cement ratio, temperature, and additives used to make the blend.

The higher the clay content, the thicker and more viscous the binder becomes since clay has a high-water demand. This may have consequences to construction projects, as it may affect the ease of pouring and spreading the cement. Another factor that influences the viscosity and flow behavior according to Ez-zaki *et al*. (2021) is the water-to-cement ratio. A higher water-to-cement ratio tends to make the cement more fluid and easier to work with, while a lower ratio results in a thicker consistency. Finding the right balance is important to ensure that the cement can be properly mixed and applied.

Temperature too plays a role in the viscosity and flow behavior of clay-based cement (Huang *et al*., 2019). Generally, higher temperatures make the cement more fluid, while lower temperatures can cause the cement to become thicker and harder to work with. Higher temperatures can accelerate the hydration reactions between water and cement particles, increasing the fluidity of the cement paste. Conversely, lower temperatures can slow down these reactions and result in thicker and more viscous pastes. The presence of clay minerals in the cement mixture can increase viscosity and thus affecting flow behavior making it hard to mix and work since it demands more water. Clays are made up of tiny plate-like particles with a high surface area, and these particles can exhibit a wide range of interactions with water, cement particles, and additives (Ferreiro *et al*., 2017). When water is added to a clay-based cement mixture, the clay minerals can absorb and retain water through hydration, swelling, and flocculation processes. This water absorption can increase the viscosity of the cement paste, making it thicker and more resistant to flow.

Furthermore, the high surface area of clay particles can also cause them to agglomerate and form a network structure, further increasing the viscosity and reducing the fluidity of the cement paste. The water-to-cement ratio can also influence the flow behavior of clay based cement. Higher water-to-cement ratios generally result in more fluid and less viscous cement pastes, as there is more water available to hydrate the cement particles and reduce the interactions between clay particles (Gao *et al*., 2015; Zhao *et al*., 2020).

In research published by Nair *et al.* (2020), they examined the rheological properties of cementitious pastes made using LC^3 vs Portland – Fly Ash 30% (FA-30) Cement and Ordinary Portland Cement (OPC) using w/c values of 0.35 and 0.40. They observed that viscosity decreased as the w/c ratio rose. For the water-to-cement ratio of 0.35, both OPC and FA-30 exhibited shear-thinning behavior whereas LC^3 paste had a distinct pattern with nearly constant viscosity when shear rates increased.

This is explained by LC3's very cohesive character, which results from its great fineness. It was determined by the investigation that the flow behavior of LC^3 was shear-thinning, like OPC and FA-30, when the w/c ratio grew from 0.35 to 0.40. Other studies Ruviaro *et al*. (2023); Spat *et al*. (2023); Tambara Júnior *et al*. (2023) that investigated the effect of Water Treatment Plant Sludge (WTPS) (0–30% wt) and eggshell filler (0–15% wt) as replacements for clay and limestone in the LC^3 system, reducing the extraction of natural resources and negative environmental impacts of waste. The results illustrated that the main dominant factor was the WTPS content due to its high surface area, roughness, and surface charge of the particles. The rise in WTPS content progressively raised the Dynamic Yield Stress (DYS) compared to the plain paste (REF). The same pattern was seen for the Static Yield Stress (SYS). This can be explained by the higher Surface Area of WTPS compared to PC, increase

in SP demand with increasing WTPS content, and irregular morphology of values of viscosity rise with rising WTPS replacement content. Since the density of WTPS is lower than that of PC, substitution by weight leads to a larger volume concentration of solids, which gradually raises the cement pastes' rheological characteristics as the PC substitution content by SCM increases (Spat *et al.*, 2023).

In another study by Ruviaro *et al*. (2023) and Scolaro *et al*. (2022), effects of Oat Husk Ash (OHA) content on the rheological properties were studied by evaluating the shear stress and viscosity at various rates of shear. The results illustrate that the increase of PC replacement content by OHA gradually increased the viscosity of the cement pastes, which is related to the elongated, angular and rough shape of OHA particles. Also, all cement pastes showed a shear-thinning response in the evaluated range, i.e., a progressive reduction in viscosity with the increase in the shear rate.

Results are in agreement with Hou *et al*. (2021), Muzenda *et al*. (2020) & Qinfei *et al*. (2019) since they reported similar results regarding the influence of calcined clay and limestone on rheological properties in LC^3 systems. In general, clay that is calcined increases static and DYS, initial thixotropic index, and viscosity (Ruviaro *et al*., 2023; Spat *et al*., 2023; Tambara Júnior *et al*., 2023). Muzenda *et al*. (2020b) illustrates that the rheological property of LC^3 differs widely from that of OPC paste. With a rise in SCM content, there is a rise in plastic viscosity, static and DYS, cohesion and adhesion, and a decrease in harmonic distortion. These investigations demonstrate that there is an increase in viscosity as the amount of SCM is increased leading to a decrease in the flow ability of material.

2.8.2 Yield Stress and Thixotropy

Thixotropy is defined as a decrease in viscosity when shear is applied, accompanied by a slow recovery when shear is removed (Bouglada *et al*., 2021). Also, it is a property of certain materials to exhibit a time-dependent change in viscosity when subjected to shear stress. Yield stress is the least amount of force needed to start a flow. Yield stress, as it relates to cement, is the amount of stress needed for the material to begin to flow or to begin to deform under load. When it comes to evaluating the performance and suitability of blended binders in different building applications, the qualities of yield stress and thixotropy are crucial. (Chen *et al*., 2021; Gao *et al*., 2015). The Yield Stress (YS) of a blended cement can be affected by elements like the types and proportions of SCMs used, water-cement ratio, and any admixtures or additives present (Li *et al*., 2022). Thixotropy is particularly important in applications such as self-leveling concrete, where material needs to flow easily during placement but maintain stability and resist segregation once in place.

Blended cement's thixotropy and yield stress can be influenced by various factors, including the type and proportion of SCMs, the fineness and PSD of the cementitious materials, the water-cement ratio, and the availability of any chemical admixtures (Jiao *et al*., 2021). The type and proportion of SCMs used in blended binders can have a significant impact on thixotropy. For example, fly ash or slag can contribute to thixotropy due to their rehydration and reconstitution processes. These materials undergo chemical reactions with water, resulting in changes in the microstructure and rheological properties of the cement paste. The amount of supplementary cementitious materials used can affect the extent of thixotropy, with higher proportions typically leading to greater thixotropic behavior (Muzenda *et al.*, 2020b). According to Hou *et al*. (2021b); Qinfei *et al*. (2019) the incorporation of SCMs like calcined

clay and limestone in cement blends improves the workability of the concrete mixture by reducing its viscosity under stress. This makes the mixture easier to place, shape, and finish, leading to improved construction efficiency and quality.

Workability is a critical aspect of cement blends, and understanding their thixotropic conduct can provide details about ease of handling, placing, and water/cement ratio requirement, their performance, and application. Thixotropy influences various aspects of cementitious materials, including mixing, pumping, and finishing. By incorporating supplementary cementitious materials such as calcined clay and limestone into cement blends, Hou *et al.* (2021) found that the thixotropic behavior of the resulting materials was affected. Thixotropy can improve the workability of cement making it easier to handle and offer better control over allowing for precise deposition and layering of material. However, thixotropic materials exhibit time-dependent behavior which requires precise timing and scheduling during application to optimize performance. Understanding the mechanisms that dominate thixotropy in cementitious materials can aid in maximizing their effectiveness and enhance their workability. The fineness and PSD of the cementitious materials also influence thixotropy. Finer particles provide more surface area for interaction with water, leading to increased rehydration and reconstitution processes (Roussel, 2012).

A study by Ruviaro *et al*. (2023) which utilized the use of Oat Husk Ash to make a blended cement, revealed that an increase of PC replacement by OHA gradually increased the dynamic yield stress of the cement pastes and eventually showed that the dynamic yield stress slowly rose with an increase in OHA replacement content. They estimated thixotropy from the area difference between the increasing and decreasing flow curves as reported by (Scolaro *et al*., 2022). In another study by Li & Fan (2022) they evaluated the thixotropy of Nano-Metakaolin

(NMK) cement pastes, the effects of superplasticizer, hydration time and environmental temperature. They concluded that:

1) The incorporation of NMK increased the thixotropy of freshly prepared cement with and without superplasticizer addition.
2) NMK significantly enhanced the cement pastes' thixotropy with superplasticizers.
3) Thixotropy of NMK cement pastes firstly increased and then decreased within 10–45˚C.
4) The maximum thixotropy temperature appeared at around 25–30˚C.
5) The thixotropy of the NMK cement pastes exhibited an increasing trend with the hydration time.
6) With an increase in yield stress, thixotropy of NMK cement pastes rose linearly.

Similar observation has been made by Zhao *et al*. (2020), thixotropy can be well improved by addition of metakaolin, and the correlation between thixotropy and structure deformation of 3D-printed CSA cement paste further proved that the improved thixotropy is beneficial to 3D- printed structural build-up. Hou *et al*. (2021a) related the mechanisms dominating thixotropy in LC^3 paste and found that LC^3 cement pastes are more flocculated than the reference sample (OPC). Contradicting information by Ez-zaki *et al*. (2021) showed that the absence of SCMs in the paste caused an unanticipated drop in the thixotropy index and static yield stress, which is explained by the shearing-induced rupture of the particle-to-particle bridge (CSH).

2.8.3 Time - dependent properties

Time-dependent refers to changes in the material's flowability and rheological behavior over time. These properties can be influenced by the addition of calcined clays as supplementary cementitious materials in the cement (Sposito *et al.*, 2022). The efficiency of superplasticizers

in dispersing blended systems with calcined clay can vary depending on the type of phyllosilicate in the clays and the type of polycarboxylate-based superplasticizer used (Chen *et al.*, 2020; Gao *et al.*, 2015).

Ez-Zaki *et al*. (2021) compared the performance of ordinary Portland cement, a combination of limestone and calcined clay and found that the low percentage of clinker in binders containing supplementary cementitious materials resulted in a longer initial setting time. They further show that in comparison to the reference binder, the use of a high calcined clay percentage in binary systems resulted in an overall setting time delay, while the equivalent substitution of limestone or limestone/calcined clay for the clinker fraction resulted in a reduced setting time delay. The explanation for the variation in the setting when supplementary cementitious materials are present includes chemical equilibria, increasing flocculation, and water demand. Although the inclusion of limestone improves the fluidity of the fresh pastes, the presence of calcined clay promotes particle flocculation.

It was reported by Dixit *et al*. (2021) that dynamic yield stress together with plastic viscosity from the rheometer tests were the same when they compared the performance of ordinary Portland cement, Portland pozzolana cement and limestone calcined clay cement with fly ash. Superplasticizer was utilized for all mixes with 60% replacement for uniformity of testing, it caused high flowability and segregation in mix results demonstrating the degradation of rheology in Limestone and Clay mixes due to calcined clay, while the Limestone Clay and Fly ash blend showed better performance due to FA. Dynamic yield stress calculated from the Bingham model showed the highest values for LC^3 blends for both the replacement regimes. All these studies are in agreement that the rheological properties of blended binders depend on the time measurement taken.

2.9 Characterization Techniques for Cementitious Materials

2.9.1 X-Ray Fluorescence (XRF)

X-ray Fluorescence (XRF) is an analytical technique used to determine the elemental composition of materials in terms of oxide. The fluoresced X-rays from the sample are collected and displayed with either energy dispersive or wavelength dispersive detector systems (Verma, 2007). The elements are identified by the wavelengths (qualitative) of the emitted X-rays while the concentrations of the elements present in the sample are determined by the intensity of those X-rays (quantitative). When an electron is ejected from an inner shell of an atom an electron from a higher shell drop into this lower shell to fill the hole left behind. This results in the emission of an X-ray photon equal in energy to the energy difference between the two shells.

High-energy X-ray photons are directed at the sample and this ejects the inner shell electrons. The principle of X-ray fluorescence technique is to excite the atoms of the substance to be analyzed by bombarding the sample with sufficiently energetic X-rays/γ-rays or charged particles. The photoionization for XRF of inner shell electrons is produced by the photons and charged particles. When this interaction removes an electron from a specimen's atom, frequently an electron from an outer shell (or orbital) occupies the vacancy. The distribution of electrons in the ionized atom is then out of equilibrium and within an extremely short time (∼10−15 s) returns to the normal state, by transitions of electrons from outer to inner shells. When an outer shell electron occupies a vacancy, it must lose a specific amount of energy to occupy the closer shell of more binding energy.

Each of such electron transfer, for example from the L-shell to the K-shell, represents a loss in the potential energy of the atom when released as an X-ray photon, the process is X-ray

emission. This energy appears as a photon (in this case a Kα photon) whose energy is the difference between the binding energies of the filled outer shell and the vacant inner shell. In the normal process of emission, an inner-shell electron is ejected producing the photoelectron. Similarly, in the ion–atom collisions one or more of the atomic electrons can get free (single or multiple ionization), one or several electrons can be transferred from one collision partner to the other, one or both of the collision partners can become excited and a combination of these elementary processes can also take place. The excess energy is taken away by either photon (characteristic X-rays), when an electron from a higher-level falls into the inner-shell vacancy or Auger (higher-shell) electrons, when the energy released during the process of hole being filled by the outer shell electron is transferred to another higher-shell electron. These emissions have characteristic energies determined fundamentally by the binding energy of the levels. The fraction of radiative (X-ray) decays is called the fluorescence yield and is high for deep inner shells. The de-excitation process leads to the emission of characteristic X-rays as shown in Figure 2.2.

Figure 2.2

The working principle of X-ray fluorescence

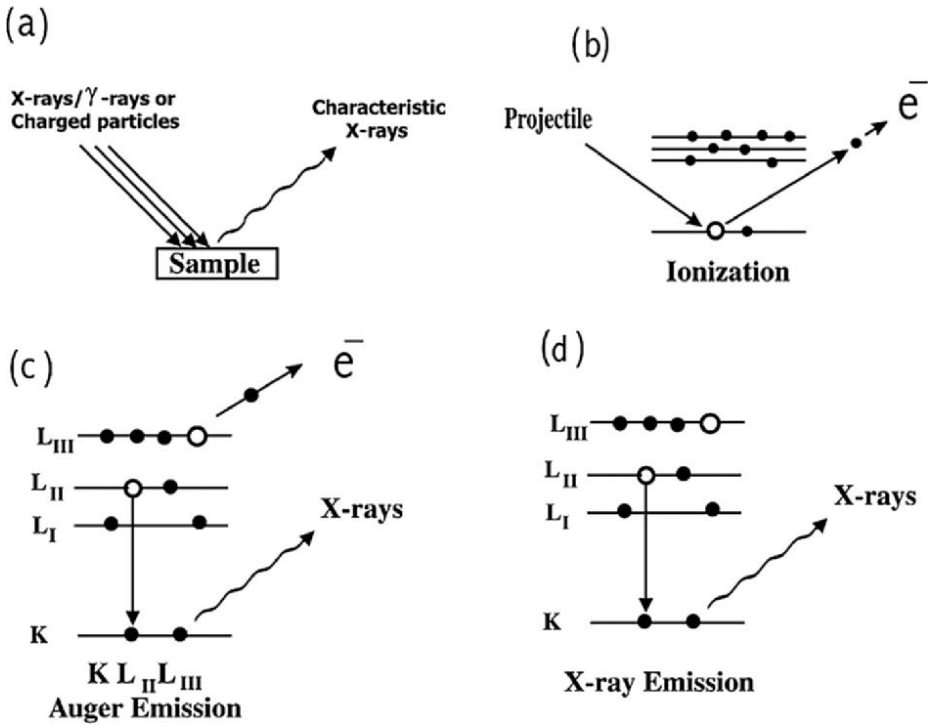

Note: (a) Schematic of the phenomenon of X-ray emission (b) Vacancy creation in the inner shell by X-rays or charged particles (c) process of Auger electron emission comprising of de-excitation and emission of higher-shell electron (d) process of X-ray emission.

2.9.2 X-Ray Diffraction (XRD)

X-ray diffraction (XRD) is an analytical technique used to determine the crystallographic structure, phase composition and microstructural properties of materials. It operates based on the principle of Bragg's Law, which describes the constructive interference of X-rays scattered by parallel planes of atoms in a crystalline material (Ermrich & Opper, 2011). According to Bragg's equation, given by $n\lambda = 2d \sin \theta$, where n is the order of diffraction, λ is the wavelength of the incident X-ray, d is the interplanar spacing and θ is the diffraction angle, XRD allows for precise identification of crystal structures by analyzing the angles at

which X-rays are diffracted. This fundamental principle makes XRD a crucial tool in cement and concrete research particularly for studying phase transformations, hydration products and the effects of supplementary cementitious materials.

The instrumentation of XRD consists of several key components that work together to generate, direct and detect diffracted X-rays. The primary component is the X-ray source which typically includes an X-ray tube containing a target material such as copper (Cu). High-energy electrons bombard this target, producing characteristic X-ray radiation, with Cu-Kα radiation (wavelength 1.5418 Å) being the most commonly used in cementitious material analysis due to its optimal energy. The emitted X-rays pass through monochromators and collimators which filter and direct the X-ray beam to ensure coherence and eliminate unwanted wavelengths.

The sample stage holds the material to be analyzed, which is typically ground into a fine powder to ensure random orientation of crystallites. In powder XRD, the most commonly used method for cement and concrete materials, the sample is scanned over a range of angles to generate a complete diffraction pattern. A goniometer controls the movement of both the X-ray source and the detector in a θ-2θ configuration, ensuring precise angular alignment. As the sample is exposed to the X-ray beam, diffraction occurs when the atomic planes satisfy Bragg's Law, producing distinct peaks at specific angles.

The detector often a scintillation counter, silicon strip detector or charge-coupled device (CCD) camera, captures the diffracted X-rays and converts them into electronic signals. These signals are processed and displayed as an intensity versus 2θ diffraction angle plot known as a diffraction pattern. Each peak in the pattern corresponds to a specific interplanar spacing (d-spacing) which is characteristic of a particular crystalline phase. By comparing the diffraction

pattern with reference databases such as the International Centre for Diffraction Data (ICDD) different phases in the material can be identified. Quantitative phase analysis can be performed using techniques like Rietveld refinement, which helps determine phase proportions, crystallite size and lattice strain (Verma, 2007).

XRD plays a critical role in cement and concrete research, particularly in identifying and quantifying phases such as alite (C_3S), belite (C_2S), ettringite, portlandite, dolomite/calcite and clay minerals like kaolinite and quartz among others. It is widely used to study the hydration process, assess the reactivity of SCMs and monitor phase transformations over time. By providing insights into the microstructural evolution of blended cement, XRD helps researchers optimize formulations for improved performance and sustainability. Furthermore, its ability to detect amorphous and crystalline phases makes it complementary to other techniques such as X-ray fluorescence (XRF) for elemental composition analysis and scanning electron microscopy (SEM) for morphological studies.

2.9.3 Scanning Electron Microscopy coupled with Energy Dispersive X-ray (SEM-EDX)

The scanning electron microscope (SEM) is an instrument that creates magnified images which reveal microscopic-scale information on the size, shape, composition, crystallography and other physical and chemical properties of a specimen (Goldstein et al., 2020.). Scanning electron microscopy is a powerful imaging and analytical technique used to study the surface morphology and composition of materials at high resolution.

The instrumentation of an SEM includes an electron gun which generates a beam of high-energy electrons typically using a tungsten filament, a lanthanum hexaboride (LaB6) cathode or a field emission gun (FEG) for higher brightness and resolution. The electron beam is

focused and controlled by a series of electromagnetic lenses, including the condenser lens and the objective lens, which reduce the beam diameter to a fine spot and direct it onto the sample surface. The sample is mounted on a stage within a vacuum chamber, as the electron beam requires a vacuum to propagate without scattering. The stage can move in multiple directions (x, y, z, tilt and rotation) to allow precise positioning of the sample.

Detectors are used to collect signals generated by the interaction of the electron beam with the sample. These include secondary electron detectors for surface topography imaging, backscattered electron detectors for compositional contrast and energy-dispersive X-ray spectroscopy (EDS) detectors for elemental analysis. The signals are processed and displayed on a monitor, forming a detailed image of the sample surface. The working principle of a scanning electron microscope is based on the interaction of the focused electron beam with the sample.

When the high-energy electrons strike the sample, they interact with the atoms in the material, producing various signals, including secondary electrons, backscattered electrons, and X-rays. Secondary electrons are low-energy electrons ejected from the sample surface, providing high-resolution topographic information. Backscattered electrons are high-energy electrons reflected from the sample, offering contrast based on atomic number, which is useful for distinguishing different phases or elements.

X-rays are emitted due to the relaxation of excited atoms and are used for elemental analysis via EDS. The electron beam is scanned in a raster pattern across the sample surface, and the intensity of the detected signals is mapped to create a detailed image. The resolution of SEM depends on the beam diameter, the interaction volume of the electrons with the sample, and

the type of signal detected. Modern SEMs can achieve resolutions down to the nanometer scale, making them indispensable for studying the microstructure of materials in fields such as materials science, biology, geology, and nanotechnology.

CHAPTER THREE: RESEARCH METHODOLOGY

3.1 Materials

3.1.1 Sample collection

Sample materials were clinker, dolomite, limestone, and gypsum which were commercially obtained and provided by the University of Padova. Two types of clay were sampled. One type was obtained from (0° 39' N, 34° 51' E) Lugari, Kakamega-Kenya and labeled A. The second one was sampled from a mining dump site in Kwale-Kenya and labeled B. The maps for the two sites are as shown in Appendix II. The choice of the two types of clay was based on their diverse mineral compositions and physical properties which offer opportunities to tailor the performance of the blended cement, thus enhancing attributes such as strength and workability.

3.1.2 Sample pretreatment

Each of the collected clay was pre-heated in an oven at a temperature of 100℃ until a constant mass was attained. After cooling, dry clay was grounded using a laboratory ball mill and sieved to a particle size of 45 μm then calcined at 700˚C for 4 h.

3.1.3 Mixing proportions

Binders used in the study were OPC and ternary blends incorporating clinker, dolomite/limestone, calcined clay and gypsum. OPC was prepared by mixing 95% clinker and 5% gypsum. The mixing proportions for ternary blends under studies were prepared as shown in Table 3.1.

Table 3. 1

Mix Proportion for Prepared Blends.

Identity of blend	Clinker (%)	Dolomite (%)	Limestone (%)	Calcined clay (%)	Gypsum (%)
OPC	95				5
SA-DOL	50	15		30	5
SB-DOL	50	15		30	5
SA-LIM	50		15	30	5
SB-LIM	50		15	30	5

3.2 Methods

3.2.1 Chemical and mineralogical compositions

The oxide composition was evaluated using an X-ray fluorescence machine (model skyray-edx3600b). 20 g of finely ground powder of each sample was weighed, pelletized and then irradiated in an X-ray fluorescence machine to determine their elemental composition. The mineralogical composition of powdered samples was determined using X-ray diffraction (Malvern Panalytical machine). About 7g of grounded powder dolomite and clay was weighed, placed in a sample holder to make a pellet using the backfilling method and then irradiated in an X-ray diffractometer. Data was collected from 20˚to 60˚2-theta range with a 2.90 seconds time step, utilizing Cu-Kα X-ray radiation with a wavelength of 1.7890 Å.

3.2.2 Standard consistency

Standard consistency was determined using a Vicat apparatus that has a plunger and needle. About 300 g of each cement was weighed accurately using a balance and 25% of water added

(75 ml) using a granulated beaker. Weighed blend and water were placed into a bowl and immediately a mixer machine started at a low speed of 140 rpm while starting the timer. The mixer was stopped after one and a half minutes for 30 seconds, during which removal of adhering pastes was done using a rubber scraper and positioned in the bowl's center. The mixer was restarted and ran at low speed for another 90 seconds. The paste was immediately transferred to a lightly oiled mold and filled up to excess without undue compaction or vibration. Voids in the paste were removed by gently tapping the slightly overfilled mold against the ball of the hand. The excess paste was removed by a gentle sawing motion using a flat trowel to create a smooth upper surface.

The Vicat apparatus was adjusted manually by lowering the plunger to rest on the base plate used and adjusting the pointer to read zero. Immediately after leveling the paste, mold was transferred to the base plate and then placed centrally under the plunger in the Vicat apparatus. The plunger was lowered gently until it was in contact with the paste. Moving parts were released and the plunger was permitted to reach the paste's center vertically. Thirty seconds after the plunger was released, the scale was read and the paste's water content was noted. The plunger was then cleaned and the procedure was repeated with pastes containing varied percentages of water content at an interval of 2% until the distance between the plunger and base plate was 7 mm. At this point, the water content used was noted as the water required for consistency.

3.2.3 Cement soundness

Cement paste was made following KS EAS 148-3 2017, which specifies standard consistency. Without compacting it too much, the paste was poured into a Le Chatelier mold that had been lightly lubricated. The mold was covered with a cover plate that was gently greased and left

for about 24 hours in a room with a humidity level of 90%. After measuring the distance (A) between the indicator points, the mold was gradually heated to boiling for 30 minutes and the water bath was kept at that temperature for 3 hours. After boiling, the separation (B) between the indication points was measured. After removing the mold from the heat and leaving it to cool, the distance (C) between indicator points was calculated. Cement soundness was determined by calculating the difference between C and A.

3.2.4 Setting time: initial and final setting time

Vicat molds were filled with cement paste (of water of normal consistency) according to KS EAS 148-3 2017. After positioning the mold, base plate and container beneath the Vicat apparatus's needle, the needle was gradually lowered until it made contact with cement. The moving positions were released and the needle was permitted to pierce a paste vertically. Thirty seconds after the needle was released, the scale was read and recorded. At intervals of 10 minutes, the identical process was carried out on the same specimen with a minimum distance of 5 mm between each other and 10 mm from the last penetration. Time was measured from zero to the point where there was 7 mm of space between the base plate and the needle as the initial time.

According to KS EAS 148-3 2017, the mold used for the initial time was inverted and immersed in a container. The needle was lowered gently until it was in contact with the paste. Moving parts were removed and the needle was allowed to penetrate vertically into the paste then, time was recorded 30 seconds after the release of the needle. The procedure was repeated 5mm from each other at 10 mm from the last penetration at intervals of 30 min. Time was recorded from zero to time needle only penetrated 0.5 mm into the blend.

3.2.5 Mechanical properties

The protocol in KS EAS 148-1 2017 was followed to obtain the strength of the binders but with some modifications. After adding cement and water (w/c = 0.5) to a sample cup, the mixer machine was spun at 160 rpm and gradually raised to 700 rpm for three minutes to create a homogenous paste. After that, the paste was put into the mold for 24 hours at 22 ˚C in a 95% humidity chamber. After that, it was demolded and the prisms were labeled for identification. On the 7^{th} and 28^{th} days of curing, each cube was taken and allowed to drain water on a non-absorbent surface material. The specimens were taken out and split in half with a replica of the compressive strength machine (Model no. 82-P0374-Controls). The compressive strength of each half was measured and the strength recorded as the average of the two.

3.2.6 Rheology

A rheometer machine (model MCR 92, Anton Paar) with a plate-plate serrated system was used to estimate the flow properties of ternary blends after setting a 1.5 mm gap. Each ternary blended cement was accurately weighed and placed in a sample cup. W/C of 0.5 was added to make a workable paste. They were mixed for 3 minutes in a power IKA ultra turrax tube drive rotating at 1600 rpm. About 4 g of the paste was scooped and placed on the serrated plate-plate rheometer. Before the actual measurements, a pre-shear was performed at a high shear rate of 200 s^{-1} amplitude for a homogeneous state to be achieved. Rheological tests started by an increasing shear rate from 2.06×10^{-6} s^{-1} to 10 s^{-1} over 130 s and then after 5 seconds, it started to decrease. The shear stress and shear rate results from the decreasing measurements were used to calculate the yield stress and plastic viscosity in flow curves fitted by the Bingham Model (equation 3.1).

$$\tau = \tau_0 + \mu_p \dot{\gamma} \quad (3.1)$$

Where: τ- Shear stress, τ_0- yield stress, μ_p- plastic viscosity and $\dot{\gamma}$- shear rate.

3.2.7 Microstructure of hydrated paste

To determine the morphology of the hydrated paste, the unfractured paste fragments used to determine the strength were taken to analyze the hydration products formed using X-ray diffraction and scanning electron microscope. The hydration process was stopped by putting the samples in ethanol for 3 days. The samples were removed from the ethanol and dried in an oven for 30 minutes at a temperature of 40 $^{\circ}$C. Samples for X-ray diffraction analysis was powdered and micronized. The backfilling method was used to prepare samples for the X-ray diffraction analysis. The remaining samples were taken for scanning electron microscope analysis. They were pre-polished and cast in an epoxy resin, then polished again to achieve a cross-section of the sample and coated with carbon. Energy Dispersive X-ray Spectroscopy (EDS) was utilized to check the elements present in the phases observed.

CHAPTER FOUR: RESULTS AND DISCUSSIONS

4.1 Introduction

This chapter presents the results of the experimental investigation into the use of dolomite and calcined clay as Supplementary Cementitious Materials in ternary blended cement. The findings are discussed in the context of their implications for the cement industry, particularly in regions like Africa where the availability of high-quality limestone is limited. This chapter is organized as follows: First, the physical and mechanical properties results are presented and discussed focusing on the performance of dolomite-based blends compared to limestone-based blends and Ordinary Portland Cement. Through tests, key parameters such as particle size distribution, mineral and chemical composition, setting times, water demand and soundness were examined to understand the behavior of different blends containing limestone, dolomite and calcined clay. Next, the microstructural characteristics of the blends are examined using X-ray diffraction and scanning electron microscopy, providing insights into the hydration mechanisms and phase formation. Finally, the rheological properties of the ternary blends are analyzed with an emphasis on workability and flow behavior.

4.2 Characterization of Samples

The characterization techniques used to analyze the chemical composition, mineralogical phases and microstructural properties of the cementitious samples are presented here. The experiments conducted included X-ray fluorescence for elemental composition analysis, X-ray diffraction for phase identification and scanning electron microscopy for microstructural evaluation. The samples analyzed in this study included ternary blended cement formulations containing clinker, calcined clay (A and B), dolomite and gypsum. A control sample incorporating limestone instead of dolomite was also characterized for comparison. They were

labeled as SA-DOL and SB-DOL for samples having clay A/B and Dolomite respectively. For those with limestone, they were labeled as SA-LIM and SB-LIM.

The chemical composition was determined and presented in the form of elemental oxides as shown in Figure 4.1. Limestone is located in the uppermost region near CaO, which indicates its high calcium carbonate content. Dolomite appears slightly lower which aligns with its magnesium content and potential reactivity differences compared to pure limestone. This suggests that using dolomite instead of limestone could introduce different hydration reactions resulting in differences in terms of performance. Clays are located at the lower region indicating they are rich in alumina and silica. The different positions of Clay A and Clay B suggest variations in their chemical composition which could impact pozzolanic activity and interaction with calcium from limestone or dolomite.

The kaolinite peak was present in clay after running the raw data in Profex software. This is an interested mineral in all clays that are used as supplementary cementitious materials. Other minerals observed in the clays were quartz, rutile and illite. A dolomitic peak was observed for dolomite while limestone had a calcite peak. The kaolinite peaks in clay disappeared upon calcination. Clay calcination causes the kaolinitic peak to vanish since it has changed to an amorphous state (metakaolin). The X-ray diffraction results provide insight into the mineralogical composition of the raw materials. Figure 4.2 represents the X-ray diffraction results for clay and dolomite respectively.

Figure 4.1

Chemical Composition of the Raw Materials

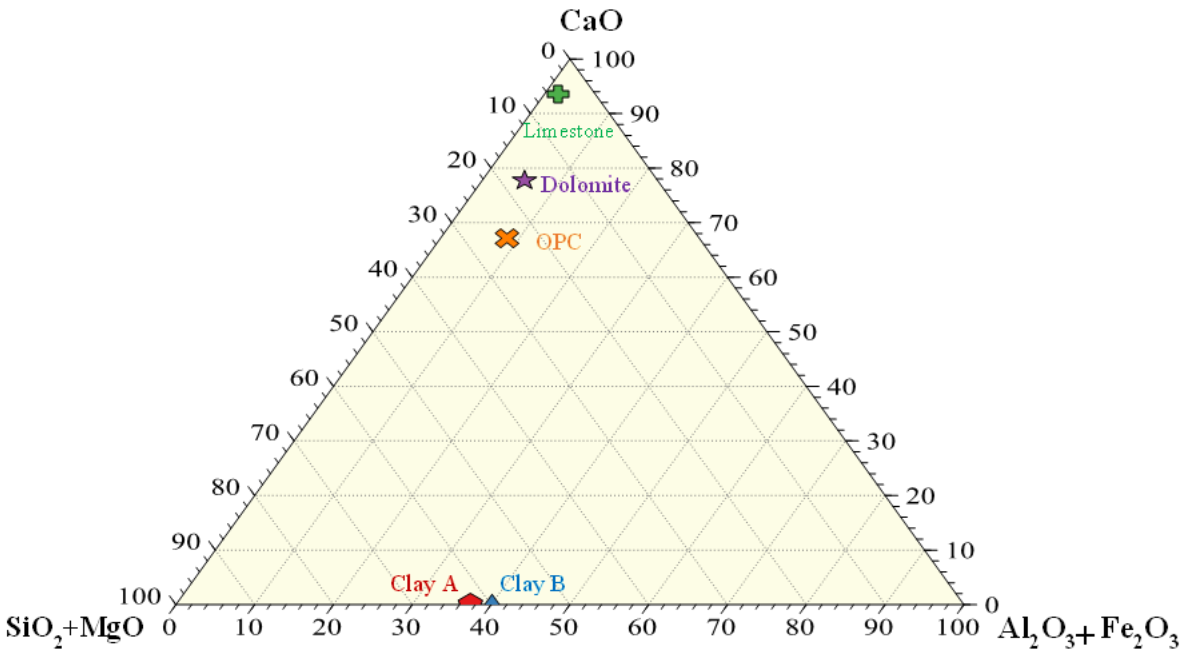

Figure 4.2

Mineralogical composition of the Raw Materials

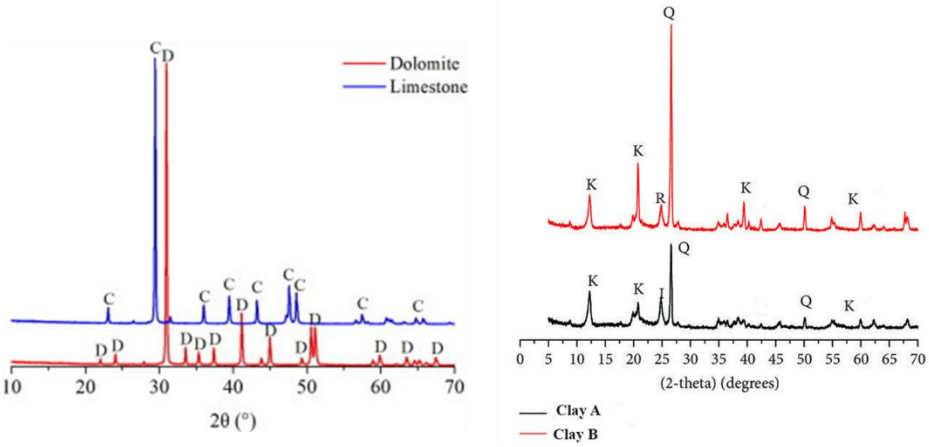

Note: C-Calcite, D-Dolomite, K-Kaolinite, R-Rutile, I- Illite, Q-Quartz

The Particle Size Distribution (PSD) for limestone, dolomite and clay A and B are shown in Fig 4.3. As the sieve size increases the percentage remaining also increases meaning that larger sieve sizes retain more material. Limestone shows a slightly higher retention at smaller sieve sizes compared to the other materials thus has a finer fraction. Dolomite has a similar distribution to limestone but with slightly coarser particles. Both clays follow a comparable trend with Clay A being slightly coarser than Clay B in the range of (30 -100 μm).

If a material has more retention at smaller sieve sizes it means it has finer particles. Based on these curves, Limestone is finer than the rest. All the curves suggest that the materials have a relatively well-graded distribution meaning they contain both fine and coarse particles. Finer particles (Limestone and Clay B) improve early strength and workability due to increased surface area. Coarser particles (Clay A and Dolomite) reduce water demand but could increase the setting time and hydration rate. The similarity of the curves shows that these materials have compatible particle size distributions which is beneficial for blending in cement production. The Particle size distribution suggests that these materials can be effectively be used to as ternary cement formulations to balance reactivity and workability.

Figure 4.3

Particle Size Distribution

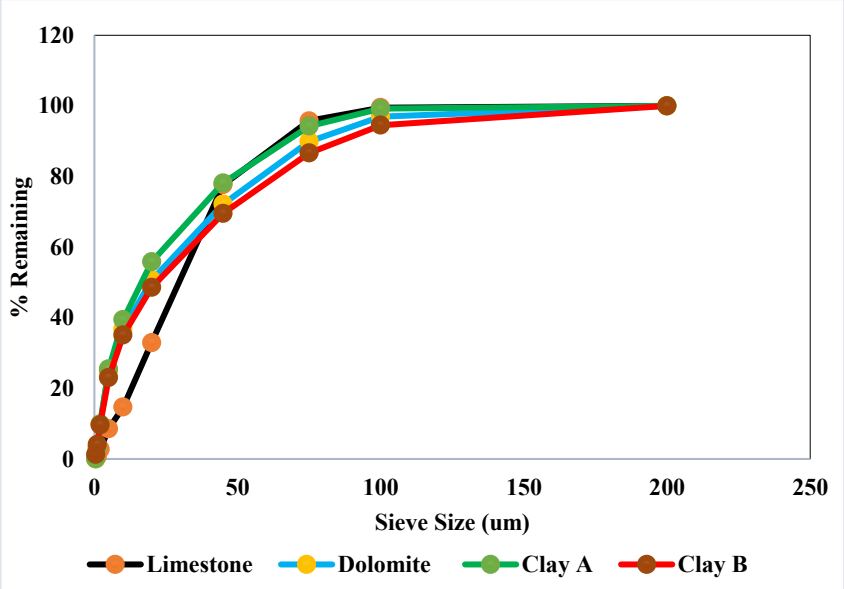

4.2 The Physical Properties of Cement Blends

Standard consistency was done to determine the amount of water needed to make a workable paste. According to the standards it should range from 26-38% of the cement used. OPC had a consistency of 26% while the ternary blends had a slightly higher water demand but still within the standard's limits. This is a result of increased surface area or fineness of calcined clay and dolomite/limestone requiring more water for proper workability.

According to BS EN 196-3:2016 Standard, the initial setting time should be greater than 45 minutes and final setting time should be less than 600 minutes. OPC sets the fastest with an initial setting time of 100 min and final setting time of 190 min. Limestone-based blends (SA-LIM, SB-LIM) had slightly delayed setting times compared to OPC. Dolomite-based blends (SA-DOL, SB-DOL) had significantly longer setting times (170 and 169 minutes as initial setting times, 304 and 310 minutes as final setting time), meaning dolomite retards the setting process more than limestone. The difference in setting times between the ternary blends is

because of the difference in PSD of the materials. The coarser dolomite tends to hydrate slowly compared to finer limestone. An increase in setting time is suitable as it facilitates adequate time to place, mix and transport concrete.

The soundness test, which evaluates volumetric stability showed that all samples meet the standard limit, meaning that no excessive expansion occurred. However, dolomite-based blends (SA-DOL, SB-DOL) exhibited slightly higher expansion, but values remained within the standard limit (1.99-2.00 mm) compared to limestone SA-LIM, SB-LIM (1.00-1.50 mm); this is possibly due to the presence of MgO in dolomite. If longer workability and setting time are required, dolomite-based blends are suitable. All blends comply with BS EN 196-3:2016 standards meaning they are technically viable for cement applications. All the physical properties determined were within the range specified by the British Standards, as shown in Table 4.1.

Table 4.1

Physical Properties of Cement Blends

	Setting times (Min)			
Identity	Initial	Final	Water demand (%)	Soundness (mm)
BS EN 196-3 2016	>45	<600	26- 38	10
OPC	100	190	26	1.00
SA-LIM	115	234	27	1.50
SB-LIM	118	230	26.5	1.00
SA-DOL	170	304	27	2.00
SB-DOL	169	310	26.5	1.99

4.3 The Mechanical Properties of the Ternary Blended Cement Formulations

The compressive strength of the samples was determined on 7^{th} and 28^{th} day to assess the mechanical performance of the ternary blended cement formulations. The results indicated variations in strength development depending on the composition of the blends. At day 7, OPC had achieved a compressive strength of 30 MPa which was the highest among all samples. The high strength observed in OPC is possibly due to the higher proportion of C_3S and C_2S which is responsible for its superior strength development. The blends containing limestone (SA-LIM and SB-LIM) recorded compressive strengths of 22 MPa and 27 MPa respectively.

These values indicate that the addition of limestone in the ternary blended system provided a favorable environment for early hydration reactions. The dolomite-containing samples (SA-DOL and SB-DOL) exhibited compressive strengths of 26 MPa and 24 MPa respectively which were lower than those of the OPC at this stage. The relatively lower early strength of the dolomite blends suggests that dolomite influenced hydration kinetics differently compared to limestone. This can be attributed to its chemical composition where the presence of magnesium carbonate ($MgCO_3$) results in delayed hydration reactions.

After 28 days, all samples exhibited increased compressive strength due to continued hydration and pozzolanic reactions. OPC recorded the highest strength of 44 MPa. The limestone-based blends (SA-LIM and SB-LIM) reached 39.5MPa and 41MPa respectively showing an approximate 13% and 15% reduction in strength compared to OPC. This suggests that while limestone and calcined clay contribute to hydration and strength development, their effect was slightly lower than that of OPC due to the dilution effect on clinker content. The dolomite-based blends (SA-DOL and SB-DOL) reached strengths of 39 MPa and 38 MPa respectively at 28 days. The strength development of these blends showed a 48-50% increase from the 7th-day values, which is higher compared to the 37-40% increase observed in limestone-based blends.

This suggests that dolomite enhances long-term strength gain possibly due to delayed secondary reactions involving $MgCO_3$ which contribute to microstructural densification. From these results it is evident that limestone enhances early-age strength development while dolomite contributes to strength gain at later ages. The slower early strength of dolomite-based blends may require modifications in curing conditions or activators to optimize its contribution to strength development.

The difference in strength can be attributed to the dilution effect stemming from the partial substitution of clinker which consequently decreases the main cement hydration phases (C_3S and C_2S) that are responsible for compressive strength development (Scrivener et al., 2018). Although OPC maintains the highest strength at both curing ages, ternary blends with limestone and dolomite exhibit comparable long-term performance making them suitable for sustainable cement production. The comparison between strength development for all the blends is as illustrated in Figure 4.4.

Figure 4.4

Compressive Strength Values

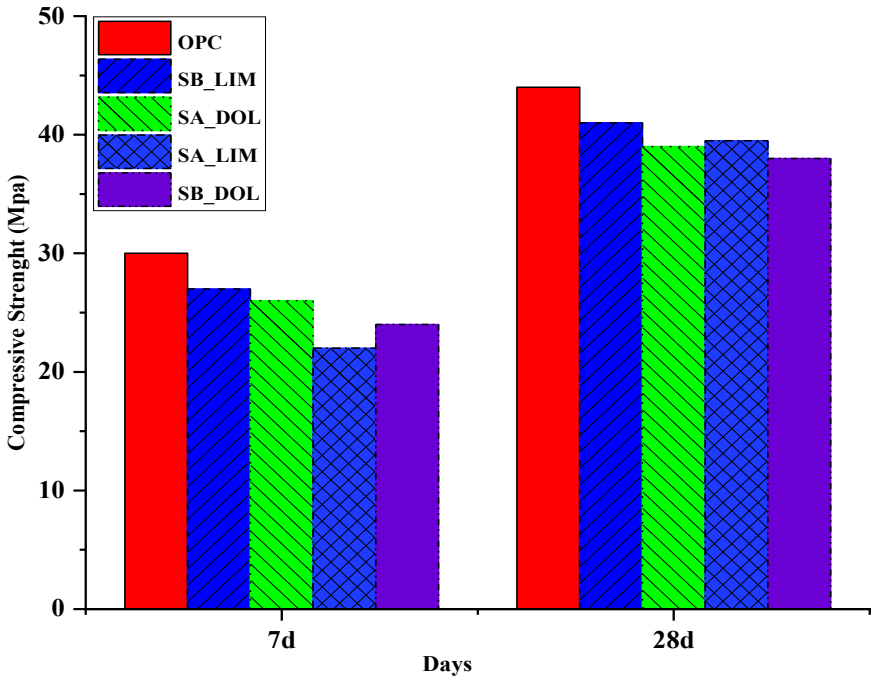

4.3.1 The efficiency factor of the ternary blends

The Efficiency factor (k-value) for all ternary blends was determined. This is a measure of the number of cement parts in a blend or concrete mixture that can be substituted with one part of

pozzolana without affecting the compressive strength performance of the binder (Wong and Razak 2005). The k - value was determined as illustrated in equation 4.1.

$$k = \frac{R_s(M_{CO}-M_C)}{M_{scm}} \quad (4.1)$$

Where k- efficiency factor, Rs - the relative strength (i.e., the strength of paste with SCM / strength of control at the same age), M_{CO}- cement content in the control, M_C-cement content in the blended mix in kg/m^3 and M_{scm}- the SCM content in the blended mix in kg/m^3.

According to Bediako and Valentini (2024); Wong and Razak (2005), if k is equal to 1 then the SCM has the same efficiency as Portland cement and therefore it can replace weight-weight basis without affecting strength. For k greater than 1, it shows that the pozzolana has a higher cementing efficiency than cement. On the other hand, if k < 1, the pozzolana is less effective than cement in terms of contributing to strength development.

The k-value for all the ternary blends (SA-DOL, SB-DOL, SA-LIM, SB-LIM) ranged from 0.5-0.7 and 0.8-1.0 on the 7th and 28th day respectively as illustrated in figure 4.5. On the 7th day, SA-LIM, SB-LIM, SA-DOL and SB-DOL had k - values of 0.56, 0.69, 0.67, and 0.61 respectively while on the 28th day, the k - values calculated were 0.90, 0.93, 0.87 and 0.86 respectively. These values are in the range for k-values of natural pozzolans. A typical increment with curing days in the k-value is observed. According to Bediako & Valentini, (2024), the k value can change with time. Enhanced k-value is attributed to the increased mechanical properties that result from the pozzolanic reaction typically as a result of silica and alumina present in the calcined clay reacting with portlandite to form additional silica gels.

Based on these findings, it can be concluded that the calcined clay and limestone can replace weight to weight basis of OPC without affecting the property being investigated. On the other

hand, the dolomite-containing blends showed a lower efficiency value. Dolomite blends are less efficient than limestone blends although they still contribute significantly to the cementitious qualities.

The k-value varies greatly depending on the type of pozzolan. From some of the studies done for instance, fly ash (FA), its k- value usually falls between 0.2 and 1.0. Because Class F FA contains less calcium than Class C FA (Yu *et al*. 2021). Silica fume is highly reactive and may greatly improve the characteristics of concrete has a k-value ranging from 2.0 to 4.0 (Okoye 2017) and slag ranges from 0.8 to 1.2. The k-value for natural pozzolans usually falls between 0.4 and 0.8 although it can vary greatly (Zunino and Lopez 2016). The efficiency factor analysis highlights that both limestone and dolomite enhance cement performance. These findings suggest that optimizing ternary blended cements with a balance between limestone and dolomite can lead to sustainable and high-performance cement formulations.

Figure 4.5

The Efficiency Factors at day 7 and 28

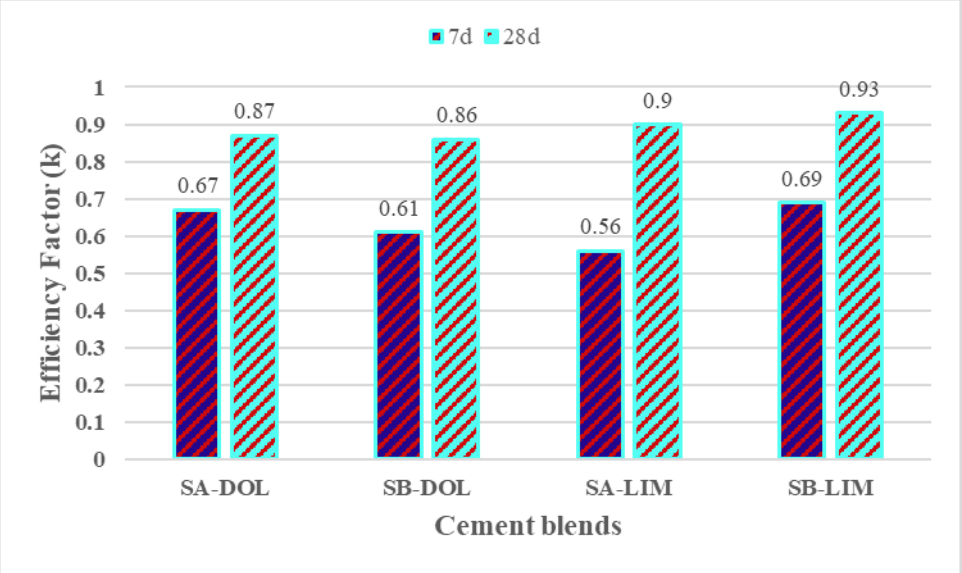

4.5 Rheology

The viscosity vs. shear rate curves for determining the ternary blend's flow properties are illustrated in Figure 4.6 a. All the ternary blends (SA-LIM, SB-LIM, SA-DOL, and SB-DOL) showed a viscosity decline as the shear rate increased. Shear-thinning property was exhibited by the blends. The shear-thinning behavior explains the chemistry of the fluid's molecules or particles as well as their interactions. Particle size distribution, Particle friction and flocculation affect particle packing, interparticle interactions and ease of alignment under shear which in turn increase initial viscosity and shear thinning behavior. Different SCMs with varying reactivity and particle properties tend to modify microstructure and hydration kinetics. More surface area interactions and simpler alignment under shear is the reason why finer particles often result in more shear thinning. The presence of clays in cement may absorb large amounts of water due to its high surface area, leading to increased viscosity and higher water demand.

Figure 4. 6

Rheological properties of the blended cement

(a)

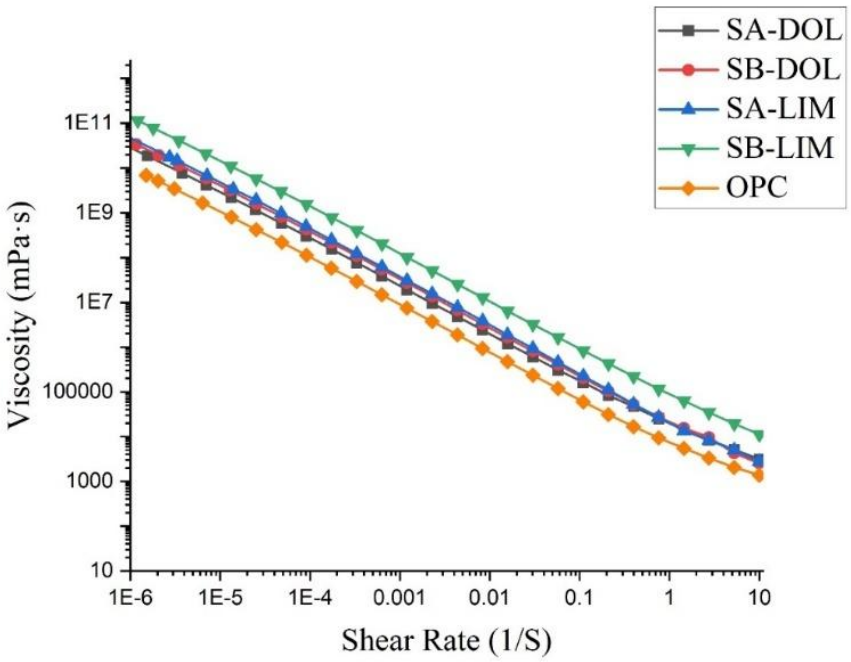

(b)

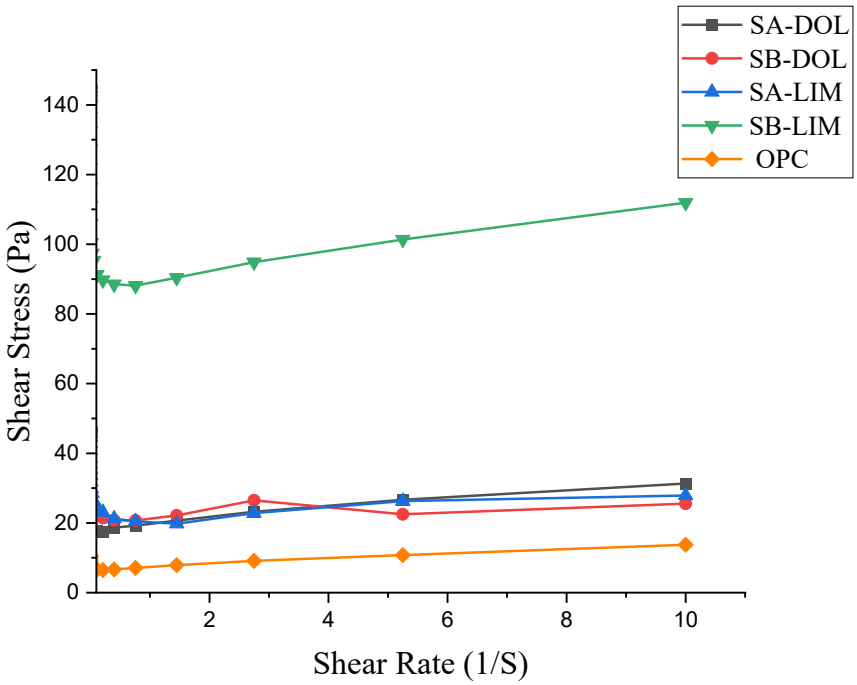

(c)

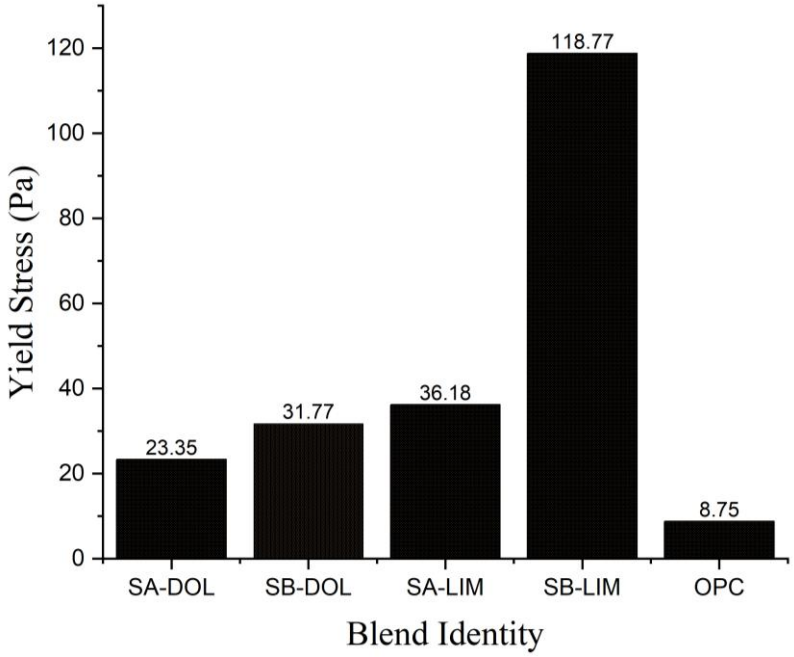

Note: (a) flow properties, (b) flow curves, and (c) yield stress of flow curves fitted by the Bingham Model.

Figure 4.6 b shows the flow curves for the ternary blended cement interpolated to get the yield points in Figure 4.6 c. In all four ternary blended cement SB-LIM was observed to have the highest yield stress by 90% suggesting the largest initial resistance to flow. This implies that at low shear rates, SB-LIM may be the thickest or most viscous paste. This could be attributed to the fact that there could be possibly extremely powerful particle-to-particle interactions resulting in flocculation. OPC had the least yield stress then followed by the samples with dolomite when compared to samples with limestone. At low yield points it implies that they might be thinner and have more fluid pastes. From Figure 4.3, dolomite is coarser compared to limestone.

According to Chateau (2012), a particulate system's yield stress (YS) rises as particle size decreases mostly because of the higher surface area to volume ratio that strengthens interparticle interactions. When combined these elements raise the flow resistance and cause systems with finer particles to have a higher YS than those with coarser particles.

The flow curves for SA-DOL and SB-DOL indicate low yield points with a steady rise throughout shear rates. This implies that very little force or shear is required to initiate flow for dolomitic ternary blends. In contrast, SA-LIM and SB-LIM show an increased steady rise in shear stress with shear rate, conforming to higher yield points than SA-DOL and SB-DOL as shown in Figure 4.6 c.

The limestone-based ternary blends have a higher initial resistance of (around 36 Pa and 118 Pa respectively). This is due to their finer particle size dispersion and interactions of calcined clay and limestone. The yield point of SB-LIM is higher than that of SA-LIM due to the difference in the reactivity of these clays. The yield point of OPC is comparatively lower by 10% thus it starts to flow at lower shear forces. At a higher shear rate it surpasses SA-DOL

and SB-DOL due to its considerable increase in shear stress with shear rate. This suggests that although OPC initially resists flow, it shows a noticeable drop in viscosity with higher shear once the yield point is exceeded.

4.6 Chemical and Microstructural Characterization

4.6.1 X-Ray diffraction (XRD) analysis

Figure 4.7 displays the X-ray diffraction peaks of the ternary blended cement systems cured after 7 and 28 days. All the ternary blended cement hydrated to form main hydration products like ettringite, portlandite (CH) and calcium silicate hydrates (CSH). The CH peaks are well-defined as a significant degree of hydration at 7 days. This suggests that alite (C_3S) and belite (C_2S) have reacted efficiently releasing $Ca(OH)_2$ as a byproduct. Intense calcite (C) peaks are observed confirming the presence of limestone.

Calcite plays a role in providing nucleation sites for CSH growth and accelerating early hydration. CSH phases are present although their intensity is lower due to their amorphous nature. On the 7^{th} day, limestone-based cement blends showed a well-advanced hydration process with higher CSH and calcite content promoting to early-age strength development. On the other hand, dolomite-based blends exhibit partial hydration of dolomite leading to brucite formation. During the hydration of dolomite blended cement, dolomite reacts with calcium hydroxide reducing its availability which could have implications for later-age strength. Both ternary blends with dolomite and limestone had quartz which was initially in clay. In SA-LIM and SB-LIM, Hemicarboaluminate (Hc) and Monocarboaluminate (Mc) are formed on the 7^{th} day. This is a result of the reaction between active alumina from C_3A with calcite. Similar results have been found in a study on the microstructure development of

blended cement by (Machner *et al.*, 2017). The formation of CSH also indicates a pozzolanic reaction of Silica and alumina of metakaolin with portlandite at early curing days.

On the 28th day, reduction of CH peaks (typically at ~18° and 34° 2θ) indicate continued pozzolanic reaction forming an additional CSH phase. There are also increased broad peaks at ~29–34° 2θ indicating higher CSH formation which increased strength. The observed Ettringite stability that is persistent at ~9-10° 2θ suggests continued sulfate reaction. There is an additional rise in the intensity of Mc and Hc in the X-ray diffraction patterns at 28 days in Figure 4.7 b. Additionally, monosulfoaluminate is formed in limestone-blended cement and the intensity of portlandite on this day was reduced because portlandite was being consumed due to a pozzolanic reaction. The formation of additional phases in blended cement shows that there is pozzolanic reaction taking place and the additional phases contribute to pore refinement. Blended cements are the suitable cements to be used since they have reduced aggressive media attacks due to reduced porosity.

Figure 4.7

X-ray diffraction representation for mineralogical composition

(a)

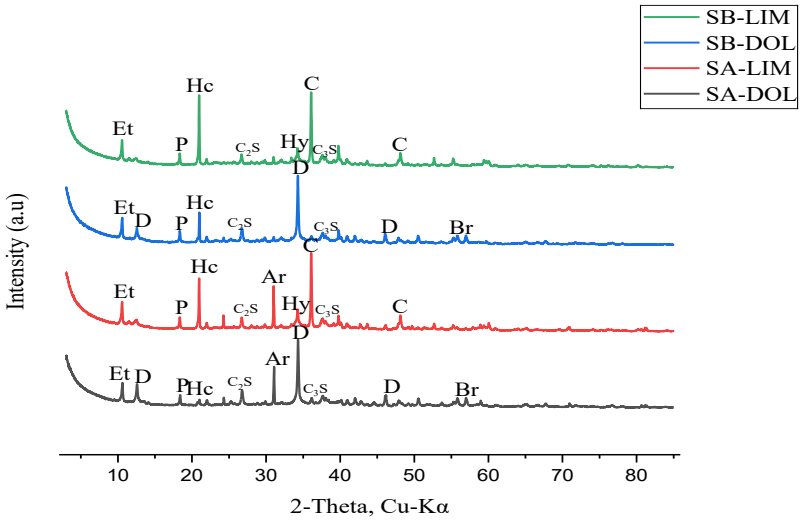

(b)

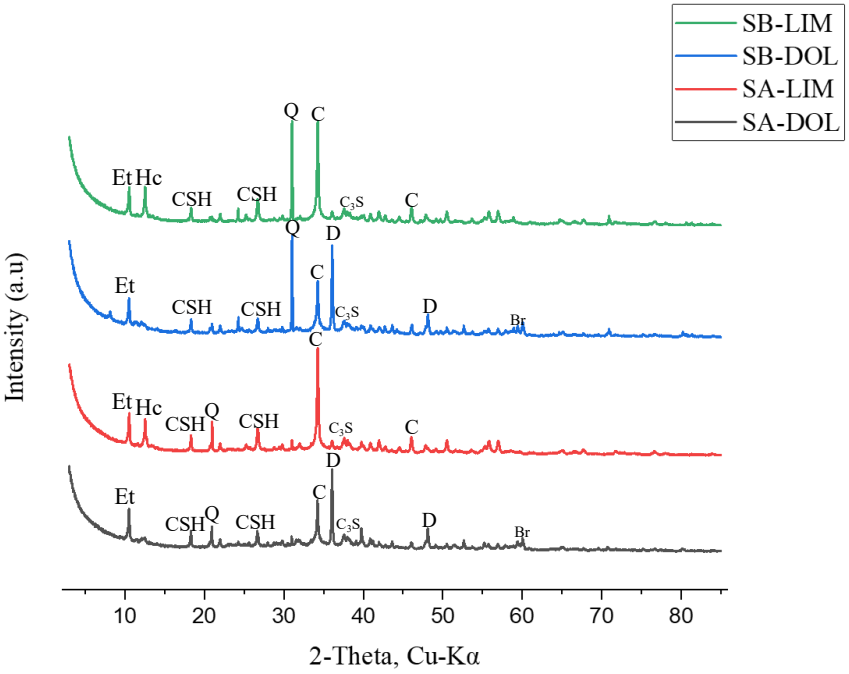

Note: (a) hydrated paste at 7 days and (b) X-ray diffraction of hydrated paste at 28 days. Et-Ettringite, Hc-Hemicarboaluminate, CSH- calcium silicate hydrate, Q- quartz, C- calcite, D-dolomite, Br- brucite.

In the ternary blend that incorporated 15% dolomite, brucite formed due to the reaction of magnesium oxide (periclase) with water (Kuenzel *et al*. 2018) (Equation 4.2). Both ternary blends with dolomite and limestone had quartz which was initially in clay. In SA-LIM and SB-LIM, Hemicarboaluminate (Hc) and Monocarboaluminate (Mc). This is a result of the reaction between active alumina from C_3A with calcite. Similar observation has been made by Qinfei *et al*. (2019) in their study. According to Athira and Bahurudeen, (2022) the calcined clay which is rich in silica and active alumina reacts with $Ca(OH)_2$ to form the CSH/CASH gel (equation 4.3). All the new phases formed can contribute to the mechanical properties of the hydrated paste. Pozzolanic reaction continues even at a later age (more than 28 days) thus blended cement gains more strength than OPC at a period between 90 days and 3 years (Zunino & Scrivener, 2021b).

$$MgO + H_2O \rightarrow Mg(OH)_2 \quad (4.2)$$

Periclase Brucite

$$CH + SiO_2 \text{ and } Al_2O_3 \rightarrow CSH \text{ or } CASH \quad (4.3)$$

The reduction in calcium hydroxide (CH) peaks over time alongside increased CSH formation suggesting pozzolanic reactivity of the calcined clays. SB-LIM and SA-LIM show higher CH consumption indicating active pozzolanic reaction and better long-term strength. SB-DOL and SA-DOL exhibit brucite (Br) formation which suggests that MgO from dolomite is hydrating potentially modifying cement microstructure and making it dense. Cement manufacturers can reduce carbon footprint by increasing the use of dolomite and limestone-based ternary blends.

4.6.2 Microstructural analysis of the hardened cement using scanning electron microscopy

A Scanning Electron Microscope was used to study the microstructure of the hardened cement pastes and assess the role of limestone and dolomite additions. The scanning electron micrographs at 1000X magnification coupled with Energy Dispersion Spectroscopy (EDS) were utilized. A difference in the porosity of the hardened cement matrices is visible whereby the blends with dolomite have a well-formed and denser microstructure compared with blends containing limestone. The predominant binder components of all the ternary blends were, ettringite, CSH, clinker phases and traces of limestone, quartz and dolomite in the blends containing those materials, respectively. These were identified by morphological features and elemental confirmation through Energy Dispersion Spectroscopy. Both blends have a dense microstructure because the hydrated dolomite and limestone act as pore refiners.

Scanning electron micrographs and energy dispersion x-rays results of the ternary blended cement mixed with dolomite and limestone with calcined clay at 28 days of curing are shown in Figure 4.8 a-d. This technique was utilized to analyze the composition, morphology and distribution of different phases present in cement paste. The ternary blends are mainly hydrated to form CSH and traces of unreacted raw material that fill the void volume to form a dense microstructure. As observed from the X-ray diffraction results of hydrated paste, the improved packing of these blended pastes is because of the higher pozzolanic influence of calcined clays (observed from portlandite consumption) and a more composite hydrate phase assemblage is the main cause of the presence of a more compact and denser microstructure in the cement matrix. Some traces of unreacted raw materials were observed as depicted by Energy Dispersion Spectroscopy.

The compactness of the microstructure and the densified cement matrix are observed since the void volume is less in all the blends. This is mostly caused by the SCM's systems' better packing and the calcined clays' increased pozzolanic effect. The Energy Dispersion Spectroscopy detected the emission of various elements, including calcium (Ca), silicon (Si), aluminum (Al), and iron (Fe) which were from the raw materials composition. The Energy Dispersion Spectroscopy results obtained revealed the composition of the mentioned elements in the cement matrix. The elements were not uniformly distributed. Fig. 4.8 displays SEM micrographs and Energy Dispersion Spectroscopy findings of the blended cement pastes which include dolomite/limestone and Calcined clay after 28 days of curing. Clinker, Dolomite/ Limestone and calcined clay are the three primary binder components that are visible in the microstructure of all four sample pastes. The bright grey un-hydrated clinker phases are observed to have a shiny speck encircled by a thin hydrated outer ring that is either dark grey or black. There is evidence of the characteristic layered structure of the calcined kaolinite phase. In line with earlier research its surface took on a fibrous structure, suggesting that it served as a fresh source of nucleation sites for the amorphous CSH phase's formation (Mutai *et al.*, 2023).

Among other phases, the formation of periclase indicates the availability of Dolomite in the microstructure. These phases indicate that none or only a tiny percentage of raw material was dissolved and thus it is acting as filler material. Given that the peaks were nearly consistent, these data correlate well with the X-ray diffraction observations obtained. The constituents of these phases (Mg, Ca, C, and Fe) are also present in the Energy Dispersion Spectroscopy data, which supports the idea that these phases were included in the binder. The unreacted clinker in all samples with CH phase visible which indicates that the pozzolanic reaction is still going

on. This agrees with previous work that shows pozzolanic reactions continue even after 28 days of curing improving the performance of blended cement.

Figure 4.8

Scanning electron microscopy images of hydrated paste.

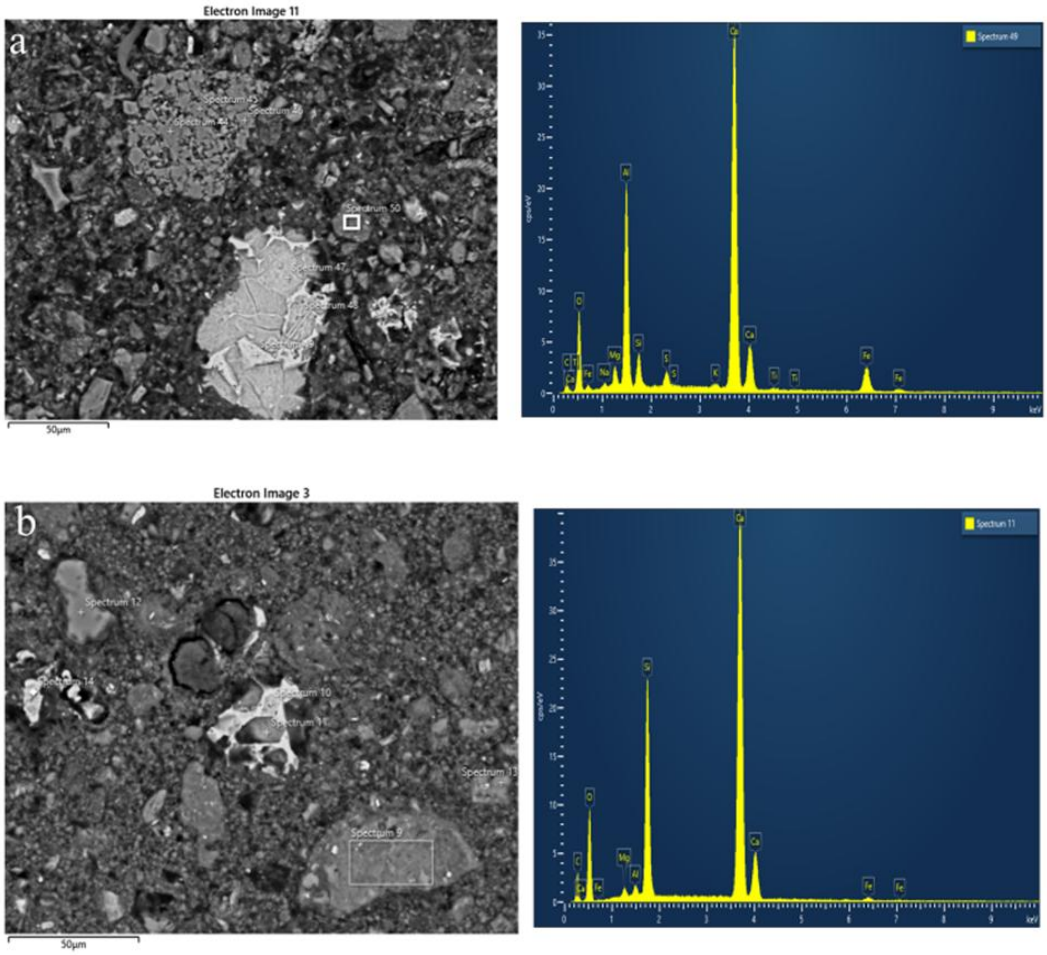

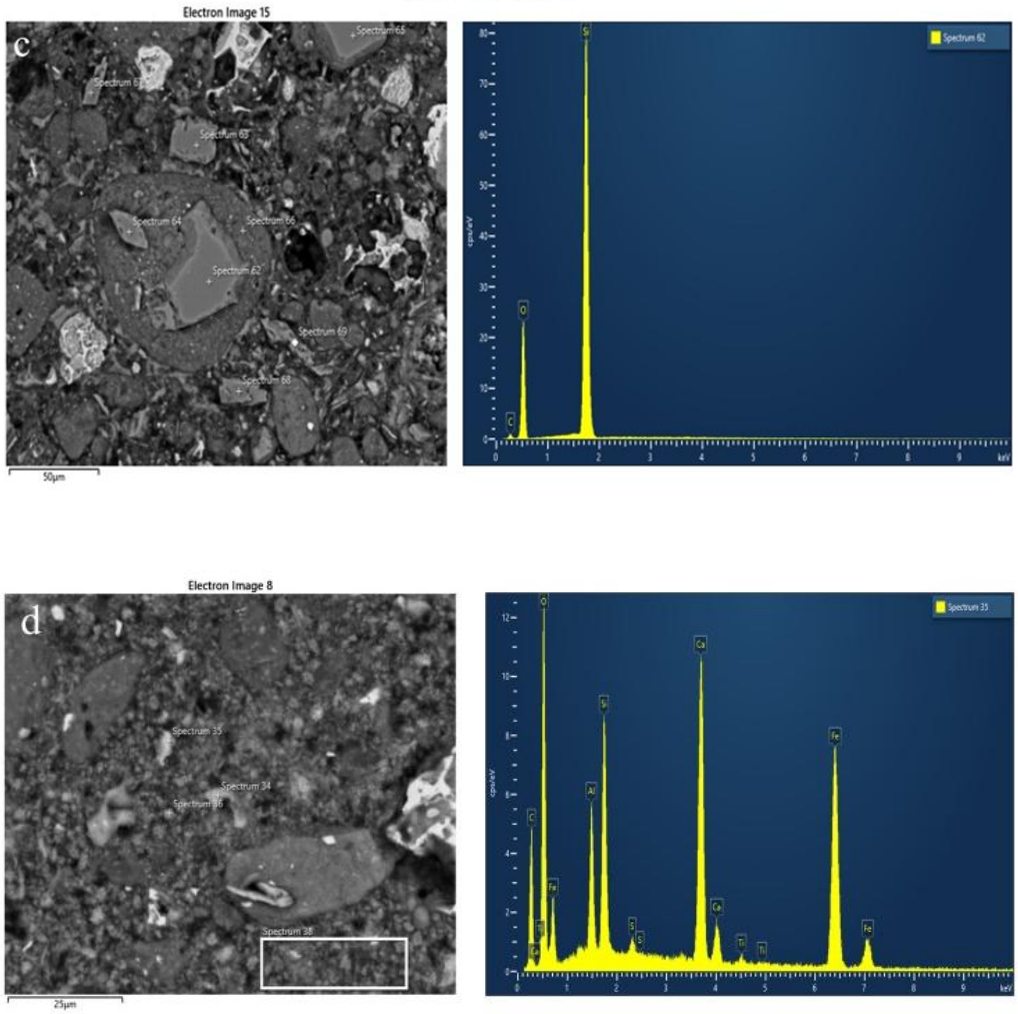

Note: (a) SA-DOL (b) SA-LIM (c) SB-DOL (d) SB-LIM

From the energy dispersion spectroscopy data, the approximate ratios of elemental composition were determined to evaluate how the pozzolanic reaction was taking place. Silicon (Si), calcium (Ca), aluminum (Al), magnesium (Mg), and sulfur (S) are present in all samples in different proportions. The Mg/Si ratios are comparatively low in all samples, suggesting that magnesium is present in lower concentrations than silicon in each sample. Samples Blended with Dolomite (SA-DOL and SB-DOL) have greater Si/Ca and Si/Al ratios. This suggests that silicon predominates over aluminum.

A greater Mg/Si ratio indicates a greater magnesium content in SA-DOL. All the blends have aluminum (Al) and S, which raises the possibility of Al-containing hydration phases like ettringite (AFt) or CAH formation. This agrees with the X-ray diffraction obtained from the hydrated paste on the 28th day. The primary binding component in cement is CSH which gives the material its strength. In an energy dispersion spectroscopy analysis (Table 4.2) a high Si/Ca (0.5 - 1.00) ratio is an indication of the possibility of abundant CSH as a result of cement hydration. Balanced aluminate and sulfate phases are suggested by the modest Al/Ca and S/Ca ratios. According to Chindaprasirt *et al*. (2012) for CaO/SiO_2 (0.24–3.20) indicates the degrading of calcium and promotes the formation of calcium aluminate silicate hydrates (CASH).

Table 4.2

Elemental Ratios from EDS

	Si/Ca	Al/Ca	Mg/Si	S/Ca	Si/Al
SA-DOL	1	0.4	0.12	0.15	2.8
SA-LIM	0.43	0.24	0.07	0.09	1.78
SB-DOL	0.67	0.34	0.08	0.13	0.54
SB-LIM	0.53	0.22	0.07	0.12	0.42

The energy dispersion spectroscopy detected the presence of various elements, including calcium (Ca), silicon (Si), aluminum (Al), and iron (Fe) which were from the raw materials composition. The energy dispersion spectroscopy results obtained revealed the composition of the mentioned elements in the cement matrix. The elements were not uniformly distributed. Figure 4.9 shows the relationship between the Al/Ca, Al/Si, and Mg/Si ratios versus the Si/Ca

ratio plotted based on the energy dispersion spectroscopy data. The plots demonstrated the approximate ratios of elemental composition determined to evaluate the global view of how the pozzolanic reaction and overall reaction in the development of the cement matrix. Si, Ca, Al and Mg are present in varying proportions in different proportions.

Figure 4.9

Graphical representation of elemental ratios from energy dispersion spectroscopy

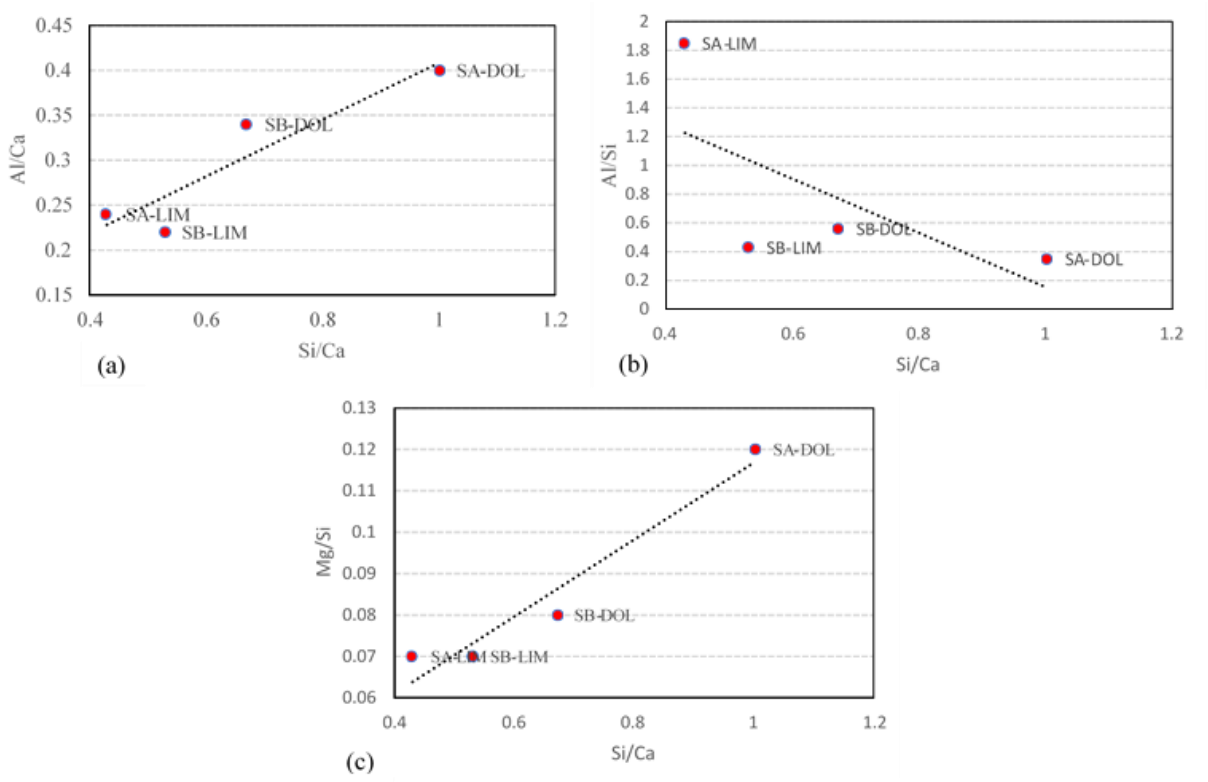

Figure 4.9 (a) shows that the dolomitic blends have higher Al/Ca and Si/Ca ratios compared to limestone ternary blends. This suggests that the dolomitic blends had more Al and Si in the cement matrix relative to Ca compared to limestone blends. This potentially explains the possible pozzolanic reaction responsible for the strength development in these blends. Additionally, reactivity of dolomites in the cement matrix as opposed to being filler material is demonstrated. On the other hand, figure 4.9 (b) shows the blends containing limestone to

have higher Al/Si at a lower Si/Ca ratio and vice versa for the dolomitic blends. Higher silicon content is associated with higher aluminum-to-silicon ratios. This phenomenon shows how different types of blend influence how Al and Si are formed into the cement matrix at varying Si/Ca ratios potentially affecting the chemical reactions and resulting properties of the cement. As expected, the Mg/Si ratios are comparatively low in limestone blends compared to dolomitic blends because dolomite has $MgCO_3$, unlike limestone which has $CaCO_3$. The greater magnesium content in SA-DOL than SB-DOL suggests higher reactivity in clay A. From these results, it is evident that calcined clays react to form additional CSH, which contributes to the mechanical properties while dolomite/limestone act as filler material. All these are suitable materials to be used as substitutes to clinker.

4.6.3 Pore refinement analysis

Pore refinement analysis was undertaken based on the 50-micron size images and compared based on the average pore size within the cement matrix. The porosity mean values were obtained from the analyzed area and rescaled based on the total area of each blend, with SA-DOL used as the reference size. Figure 4.10 shows the scanning electron microscopy images analyzed using the Fiji image processing software. The grey areas represent the cement matrix while the red region represents the pores within the cement matrix. The SEM scans show clearly the pore availability across all the blends. The pore size follows the order, SA-DOL > SB-LIM > SA-LIM > SB-DOL.

Figure 4.10

Porosity analysis of the scanned micrographs for 50 µm.

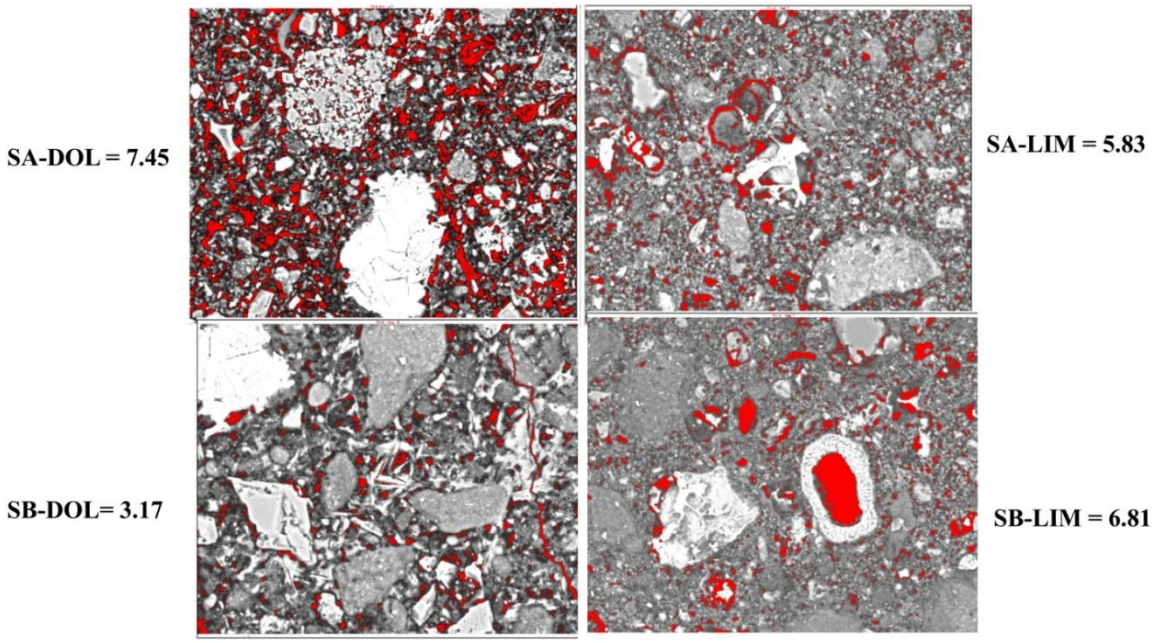

Note: The red segment represents the porosity within the cement matrix while the grey part represents the compact cement matrix.

4.6.4 Correlation analysis

The combined correlation between 28 days of compressive strength (MPa) and porosity (mean) and efficiency factor (k) is represented in Figure 4.10. The variation in the type of SCM used influences the porosity development of the hardened ternary blend. It is always expected that the pore refinement in the cement matrix contributes to higher development in the compressive strength. However, the results in Figure 4.11 demonstrate an interesting relationship between compressive strength and porosity for the ternary blended cement.

Figure 4.11

Combined correlation graph

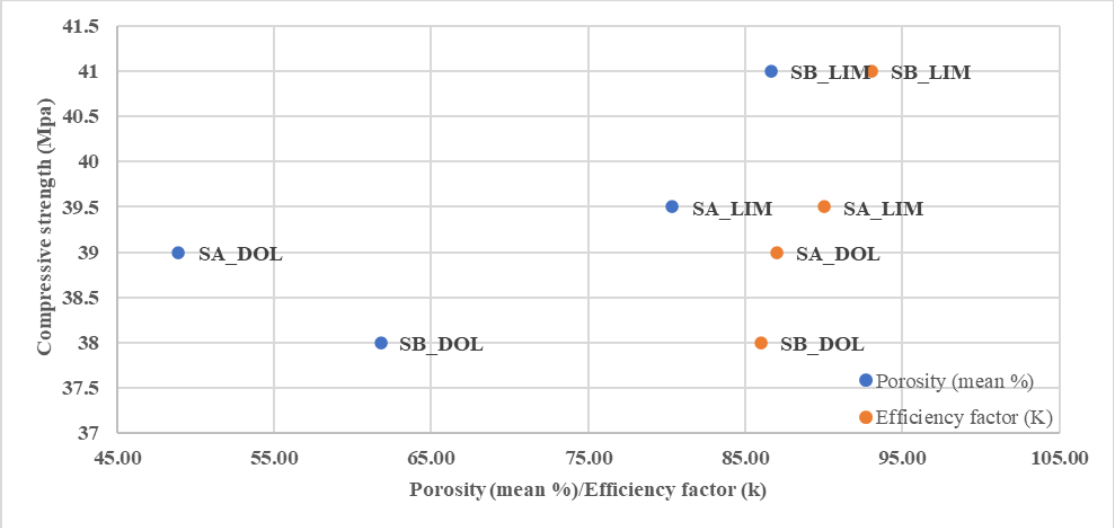

Note: display for the relationship between 28 days of compressive strength (MPa) and two different factors: porosity (mean) and efficiency factor (k).

The blended cement with higher porosity, SA-DOL (7.45%) and SB-LIM (6.81%), have higher compressive strengths (39 MPa and 41 MPa, respectively) contrary to the typical inverse relationship existing between compressive strength and porosity. In contrast, blends with lower porosity SA-LIM (5.83%) and SB-DOL (3.17%), exhibit relatively lower compressive strengths (39.5MPa and 38 MPa, respectively). On the other hand, the blends with higher efficiency factor (K) values (scaled by 100 to plot them on the same axis as porosity) are associated with lower compressive strength. However notably the SB-LIM (k = 0.93) shows the highest compressive strength (41 MPa), while SB-DOL (k = 0.86) has a slightly lower compressive strength (38 MPa). It can be concluded that factors other than porosity and efficiency factors could be contributing to higher compressive strength.

CHAPTER FIVE: CONCLUSION, RECOMMENDATIONS AND PUBLICATION

5.1 Conclusion

This study successfully produced ternary blended cement using clinker, calcined clay, dolomite, limestone and gypsum as the primary raw materials. The most significant tests conducted on the cement blends included setting time, water demand, soundness, compressive strength, microstructural analysis (XRD and SEM), and rheological characterization (flow curves and yield stress measurements).

Setting time increased with the incorporation of calcined clay, dolomite, and limestone, but all values remained within acceptable standards. This indicates a slight retardation in hydration kinetics, which can enhance workability and reduce the risk of early-age cracking.

Water demand increased, particularly in blends containing calcined clay, due to its higher surface area and pozzolanic nature. However, all blends remained within the standard limits, ensuring adequate workability.

Soundness values slightly increased across the blends but remained within permissible ranges, ensuring stability without excessive expansion.

OPC exhibited the highest compressive strength, followed by limestone-based blends, while dolomite-based blends showed a slight reduction in strength. This suggests that limestone contributed more effectively to strength gain by enhancing CSH formation, while dolomite, although reducing compressive strength slightly did not significantly impair the overall performance.

Despite minor strength reductions, all ternary blended cement met strength requirements, proving their feasibility for structural applications while supporting clinker reduction and sustainability goals.

XRD patterns confirmed the presence of portlandite, calcite, unreacted clinker phases, and amorphous content in the blends. Higher calcite and dolomite peaks were observed in dolomite-containing blends, indicating its role as a filler with limited reactivity. The presence of amorphous phases suggests pozzolanic reactions, particularly with calcined clay.

SEM images showed a dense microstructure in ternary blends, confirming the improved performance of the cement matrix. Hydration products, including C-S-H (Calcium Silicate Hydrate) gel, were observed in all blends, supporting the strength results.

Combining calcined clay and results to better performance in terms of workability compared to limestone-based blends. Limestone increases viscosity and yield stress indicating a higher water demand and potential challenges in workability. The shear-thinning nature of all blends confirms their suitability for pumpable and workable cementitious systems.

5.2 Recommendations

To build on the findings of this study, further investigation into the long-term durability of the ternary blends is recommended, particularly under aggressive environments such as sulfate-rich soils or marine conditions. This will provide valuable insights into the performance of these blends in real-world applications. Additionally, the use of superplasticizers should be considered to enhance the workability of ternary blends, especially those incorporating dolomite, which may exhibit higher viscosity. Further optimization of mix proportions is also necessary to achieve an ideal balance between workability and strength performance, ensuring that the blends meet the requirements of various construction applications.

The results of this study demonstrate that dolomite is a suitable material for use as a Supplementary Cementitious Material (SCM), as it effectively reduces porosity in the cement matrix and contributes to long-term strength development. To fully understand the hydration process, mechanical properties such as compressive strength should be evaluated at later ages, such as 90 days to determine whether hydration continues and strength gains are sustained over time. Furthermore, a detailed investigation into the mechanisms that contribute to compressive strength and porosity, such as the formation of brucite and C-S-H gel, will provide a deeper understanding of the material's performance.

Finally, the production of blended cement on a large scale should be undertaken to facilitate pre-trials of these materials in real construction projects. This will help validate the feasibility and practicality of using dolomite-based ternary blends in the industry, paving the way for their widespread adoption. By addressing these recommendations, future research can further advance the development of sustainable and high-performance cementitious materials, contributing to the global effort to reduce the environmental impact of cement production.

5.3 Publication

Masolia, C. M., Kinoti, I. K., Mureti, B., Kaigai, J., Mutua, J., M'thiruaine, C. M., & Marangu, J. M. (2025). Rheology of clay-based cement systems – a review. *Journal of Sustainable Cement-Based Materials*, *0*(0), 1–23. https://doi.org/10.1080/21650373.2025.2537268

REFERENCES

Abbass, A. M., Elrahman, M. A., Sikora, P., Strzałkowski, J., Stephan, D., & Abdel-Gawwad, H. A. (2023). From dolomite waste to katoite-based binder: Synthesis, performance and characterization. *Journal of Building Engineering*, *75*(April), 106971. https://doi.org/10.1016/j.jobe.2023.106971

Abdulqader, M., Khalid, H. R., Ibrahim, M., Adekunle, S. K., Al-Osta, M. A., Ahmad, S., & Sajid, M. (2023). Physicochemical properties of limestone calcined clay cement (LC3) concrete made using Saudi clays. *Journal of Materials Research and Technology*, *25*, 2769–2783. https://doi.org/10.1016/j.jmrt.2023.06.114

Abdunnabi, A. R. (2012). Xrf Analysis of Portland Cement for Major and Trace Elements. *Eleveth Arab Conference on the Peaceful Uses of Atomic Energy*, *December*, 23–27.

Aïtcin, P. C. (2016). Portland cement. In *Science and Technology of Concrete Admixtures*. Elsevier Ltd. https://doi.org/10.1016/B978-0-08-100693-1.00003-5

Appah, D. (2001). *Selection and use of CaO-Expanding Cements*. *19*(6), 581–591.

Athira, G., & Bahurudeen, A. (2022). Rheological properties of cement paste blended with sugarcane bagasse ash and rice straw ash. *Construction and Building Materials*, *332*, 127377. https://doi.org/10.1016/J.CONBUILDMAT.2022.127377

Bediako, M., & Amankwah, E. O. (2015). Analysis of chemical composition of Portland cement in Ghana: A key to understand the behavior of cement. *Advances in Materials Science and Engineering*, *2015*. https://doi.org/10.1155/2015/349401

Bediako, M., & Valentini, L. (2024). Strength, carbon emissions, and sorptivity behavior of cement paste and mortar containing thermally activated clay. *Journal of Building Engineering*, *89*(April). https://doi.org/10.1016/j.jobe.2024.109278

Brown, P. W. (1990). Early-Age Cement Hydration Reactions. *Transportation Research Record*, *1284*, 53–59.

Cantonati, M., Segadelli, S., Ogata, K., Tran, H., Sanders, D., Gerecke, R., Rott, E., Filippini, M., Gargini, A., & Celico, F. (2016). A global review on ambient Limestone-Precipitating Springs (LPS): Hydrogeological setting, ecology, and conservation. *Science of the Total Environment*, *568*, 624–637. https://doi.org/10.1016/j.scitotenv.2016.02.105

Cao, Y., Wang, Y., Zhang, Z., Ma, Y., & Wang, H. (2021). Recent progress of utilization of activated kaolinitic clay in cementitious construction materials. *Composites Part B: Engineering*, *211*(January), 108636. https://doi.org/10.1016/j.compositesb.2021.108636

Chateau, X. (2012). Particle packing and the rheology of concrete. In *Understanding the Rheology of Concrete*. Woodhead Publishing Limited. https://doi.org/10.1533/9780857095282.2.117

Chen, Y., Zhang, Y., He, S., Liang, M., Zhang, Y., Schlangen, E., & Çopuroğlu, O. (2023). Rheology control of limestone calcined clay cement pastes by modifying the content of fine-grained metakaolin. *Journal of Sustainable Cement-Based Materials*, *0*(0), 1–15. https://doi.org/10.1080/21650373.2023.2169965

Chindaprasirt, P., De Silva, P., Sagoe-Crentsil, K., & Hanjitsuwan, S. (2012). Effect of SiO 2 and Al 2O 3on the setting and hardening of high calcium fly ash-based geopolymer systems. *Journal of Materials Science*, *47*(12), 4876–4883. https://doi.org/10.1007/s10853-012-6353-y

Dhandapani, Y., Sakthivel, T., Santhanam, M., Gettu, R., & Pillai, R. G. (2018). Mechanical properties and durability performance of concretes with Limestone Calcined Clay

Cement (LC3). *Cement and Concrete Research*, *107*(February), 136–151. https://doi.org/10.1016/j.cemconres.2018.02.005

Di Salvo Barsi, A., Trezza, M. A., & Irassar, E. F. (2020). Comparison of dolostone and limestone as filler in blended cements. *Bulletin of Engineering Geology and the Environment*, *79*(1), 243–253. https://doi.org/10.1007/s10064-019-01549-4

Dixit, A., Du, H., Dang, J., & Pang, S. D. (2021). Quaternary blended limestone-calcined clay cement concrete incorporating fly ash. *Cement and Concrete Composites*, *123*(March), 104174. https://doi.org/10.1016/j.cemconcomp.2021.104174

Ermrich, M., & Opper, D. (2011). X-ray Powder Diffraction for the Analyst. In *PANalytical*.

Goldstein, J. I., Newbury, D. E., Michael, J. R., Ritchie, N. W. M., Scott, J. H. J., & Joy, D. C. (n.d.). *Microscopy and X-Ray Microanalysis*.

Hartmann, J., & Moosdorf, N. (2012). The new global lithological map database GLiM: A representation of rock properties at the Earth surface. *Geochemistry, Geophysics, Geosystems*, *13*(12), 1–37. https://doi.org/10.1029/2012GC004370

Hou, P., Muzenda, T. R., Li, Q., Chen, H., Kawashima, S., Sui, T., Yong, H., Xie, N., & Cheng, X. (2021). Mechanisms dominating thixotropy in limestone calcined clay cement (LC3). *Cement and Concrete Research*, *140*(November 2020), 106316. https://doi.org/10.1016/j.cemconres.2020.106316

Ijaz, N., Ye, W. M., Rehman, Z. ur, Ijaz, Z., & Junaid, M. F. (2024). Global insights into micro-macro mechanisms and environmental implications of limestone calcined clay cement (LC3) for sustainable construction applications. *Science of the Total Environment*, *907*(October 2023), 167794. https://doi.org/10.1016/j.scitotenv.2023.167794

Ijaz, N., Ye, W., Rehman, Z. ur, & Ijaz, Z. (2022). Novel application of low carbon limestone calcined clay cement (LC3) in expansive soil stabilization: An eco-efficient approach. *Journal of Cleaner Production*, *371*(April), 133492. https://doi.org/10.1016/j.jclepro.2022.133492

Jiao, W., Sha, A., Liu, Z., & Li, S. (2022). Influence of Fineness Levels and Dosages of Light-Burned Dolomite on Portland Cement Performance. *Materials*, *15*(16). https://doi.org/10.3390/ma15165798

Khelifi, S., Ayari, F., Tiss, H., & Hassan Chehimi, D. Ben. (2017). X-ray fluorescence analysis of Portland cement and clinker for major and trace elements: Accuracy and precision. *Journal of the Australian Ceramic Society*, *53*(2), 743–749. https://doi.org/10.1007/s41779-017-0087-x

Kuenzel, C., Zhang, F., Ferrándiz-Mas, V., Cheeseman, C. R., & Gartner, E. M. (2018). The mechanism of hydration of MgO-hydromagnesite blends. *Cement and Concrete Research*, *103*(October), 123–129. https://doi.org/10.1016/j.cemconres.2017.10.003

Kurdowski, W. (2014). Cement and concrete chemistry. In *Cement and Concrete Chemistry* (Vol. 9789400779). https://doi.org/10.1007/978-94-007-7945-7

Kurdowski, W., & Thiel, A. (1981). On the role of free calcium oxide in expansive cements. *Cement and Concrete Research*, *11*(1), 29–40. https://doi.org/10.1016/0008-8846(81)90006-5

Machner, A., Zajac, M., Ben Haha, M., Kjellsen, K. O., Geiker, M. R., & De Weerdt, K. (2017). Portland metakaolin cement containing dolomite or limestone – Similarities and differences in phase assemblage and compressive strength. *Construction and Building Materials*, *157*, 214–225. https://doi.org/10.1016/j.conbuildmat.2017.09.056

Marangu, J. M. (2020). *Case Studies in Construction Materials Physico-chemical properties of Kenyan made calcined Clay -Limestone cement (LC3)*. *12*.

Masolia, C. M., Kinoti, I. K., Mureti, B., Kaigai, J., Mutua, J., M, C. M., & Marangu, J. M. (2025). Rheology of clay-based cement systems – a review. *Journal of Sustainable Cement-Based Materials*, *0*(0), 1–23. https://doi.org/10.1080/21650373.2025.2537268

Mikhailova, O., Yakovlev, G., Maeva, I., & Senkov, S. (2013). Effect of dolomite limestone powder on the compressive strength of concrete. *Procedia Engineering*, *57*, 775–780. https://doi.org/10.1016/j.proeng.2013.04.098

Mutai, V. K., Marangu, J. M., M'Thiruaine, C. M., & Valentini, L. (2023). Evaluation of Kunkur Fines for Utilization in the Production of Ternary Blended Cements. *Sustainability*, *15*(23), 16453. https://doi.org/10.3390/su152316453

Ngcofe, L., & Cole, D. I. (2014). The distribution of the economic mineral resource potential in the Western Cape Province. *South African Journal of Science*, *110*(1–2), 1–4. https://doi.org/10.1590/sajs.2014/a0045

Ngui Musyimi, F., Wachira, J. M., Thiong'O, J. K., & Marangu, J. M. (2019). Performance of Ground Clay Brick Mortars in Simulated Chloride and Sulphate Media. *Journal of Engineering (United Kingdom)*, *2019*. https://doi.org/10.1155/2019/6430868

Okoye, F. N. (2017). Geopolymer binder: A veritable alternative to Portland cement. *Materials Today: Proceedings*, *4*(4), 5599–5604. https://doi.org/10.1016/j.matpr.2017.06.017

Qinfei, L., Han, W., Pengkun, H., Heng, C., Yang, W., & Xin, C. (2019). The microstructure and mechanical properties of cementitious materials comprised of limestone, calcined clay and clinker. *Ceramics - Silikaty*, *63*(4), 356–364.

https://doi.org/10.13168/cs.2019.0031

Rehsi, S. S. (1983). Magnesium Oxide in Portland Cement. In *Advances in Cement Technology*. Pergamon Press Ltd. https://doi.org/10.1016/b978-0-08-028670-9.50019-3

Roussel, N. (2012). Thixotropy: from measurement to casting of concrete. *Understanding the Rheology of Concrete*, 286–295. https://doi.org/10.1533/9780857095282.3.286

Salas, D. A., Ramirez, A. D., Rodríguez, C. R., Petroche, D. M., Boero, A. J., & Duque-Rivera, J. (2016). Environmental impacts, life cycle assessment and potential improvement measures for cement production: A literature review. *Journal of Cleaner Production*, *113*, 114–122. https://doi.org/10.1016/j.jclepro.2015.11.078

Sales, L. P. B., de Queiroz, M. G. C., da Nóbrega, A. F., da Nóbrega, A. C. V., de Souza, J. J. N., & Carneiro, A. M. P. (2021). Study of rheological properties of lime–metakaolin slurries. *Applied Clay Science*, *215*(October). https://doi.org/10.1016/j.clay.2021.106309

Scrivener, K., Avet, F., Maraghechi, H., Zunino, F., Ston, J., Hanpongpun, W., & Favier, A. (2018). Impacting factors and properties of limestone calcined clay cements (LC3). *Green Materials*, *7*(1), 3–14. https://doi.org/10.1680/jgrma.18.00029

Scrivener, K., Martirena, F., Bishnoi, S., & Maity, S. (2018). Calcined clay limestone cements (LC3). In *Cement and Concrete Research* (Vol. 114, pp. 49–56). Elsevier Ltd. https://doi.org/10.1016/j.cemconres.2017.08.017

Selman, M. M., & Ali, A. M. (2012). The Effect of Alkalis on The Properties of Portland Cement. *Anbar Journal for Engineering Sciences*, *1*(Edição Especial-Parte 1), 25–38.

Sharma, M., Bishnoi, S., Martirena, F., & Scrivener, K. (2021). Limestone calcined clay cement and concrete: A state-of-the-art review. *Cement and Concrete Research*,

149(August), 106564. https://doi.org/10.1016/j.cemconres.2021.106564

Tao, J. L., Lin, C., Luo, Q. L., Long, W. J., Zheng, S. Y., & Hong, C. Y. (2022). Leveraging internal curing effect of fly ash cenosphere for alleviating autogenous shrinkage in 3D printing. *Construction and Building Materials*, *346*(April), 128247. https://doi.org/10.1016/j.conbuildmat.2022.128247

Unluer, C., & Al-Tabbaa, A. (2015). The role of brucite, ground granulated blastfurnace slag, and magnesium silicates in the carbonation and performance of MgO cements. *Construction and Building Materials*, *94*, 629–643. https://doi.org/10.1016/j.conbuildmat.2015.07.105

Verma, H. R. (2007). Atomic and nuclear analytical methods: XRF, mössbauer, XPS, NAA and ion-beam spectroscopic techniques. In *Atomic and Nuclear Analytical Methods: XRF, Mössbauer, XPS, NAA and Ion-Beam Spectroscopic Techniques*. https://doi.org/10.1007/978-3-540-30279-7

Wang, D., Shi, C., Farzadnia, N., Shi, Z., & Jia, H. (2018). A review on effects of limestone powder on the properties of concrete. *Construction and Building Materials*, *192*, 153–166. https://doi.org/10.1016/j.conbuildmat.2018.10.119

Yamashita, M., Harada, T., Sakai, E., & Tsuchiya, K. (2020). Influence of sulfur trioxide in clinker on the hydration heat and physical properties of Portland cement. *Construction and Building Materials*, *250*, 118844. https://doi.org/10.1016/j.conbuildmat.2020.118844

Zheng, L., Xuehua, C., & Mingshu, T. (1992). Hydration and setting time of MgO-type expansive cement. *Cement and Concrete Research*, *22*(1), 1–5. https://doi.org/10.1016/0008-8846(92)90129-J

Zunino, F., Martirena, F., & Scrivener, K. (2021). Limestone calcined clay cements (lc3). *ACI Materials Journal*, *118*(3), 49–60. https://doi.org/10.14359/51730422

Zunino, F., & Scrivener, K. (2021a). Assessing the effect of alkanolamine grinding aids in limestone calcined clay cements hydration. *Construction and Building Materials*, *266*, 121293. https://doi.org/10.1016/j.conbuildmat.2020.121293

Zunino, F., & Scrivener, K. (2021b). The reaction between metakaolin and limestone and its effect in porosity refinement and mechanical properties. *Cement and Concrete Research*, *140*, 106307. https://doi.org/10.1016/j.cemconres.2020.106307

APPENDICES

Appendix A: Publication

Journal of Sustainable Cement-Based Materials, 2025
http://dx.doi.org/10.1080/21650373.2025.2537268

Rheology of clay-based cement systems – a review

Cleah Minayo Masolia[a]*, Ismael Kithinji Kinoti[a], Brian Mureti[b], Joseph Kaigai Mwangi[b], John Mutua[b], Cyprian Muturia M'thiruaine[a] and Joseph Mwiti Marangu[a,b]

[a]*Department of Physical Science, Meru University of Science and Technology, Meru, Kenya;* [b]*Institute of Cement and Concrete, Meru University of Science and Technology, Meru, Kenya*

(Received 14 February 2025; Accepted 17 July 2025)

Abstract. Cement is the world's second-most consumed material and its production contributes substantially to global CO_2 emissions. Replacing clinker with supplementary cementitious materials (SCMs), such as calcined clay, can lower the carbon footprint. Calcined clay, available in abundance and processed at 800–900 °C, can replace up to 50% of clinker. This review critically examines the rheological behavior of clay-based cement systems, focusing on their yield stress (YS), viscosity, and thixotropy. Compared to OPC, clay-based systems show a 20–70% increase in YS with >30% calcined clay, and nano-metakaolin enhances thixotropy by up to 60%. Herschel–Bulkley's model ($R^2 > 0.98$) describes best their non-linear shear-thinning behavior. While shear-thinning improves pumpability in applications like 3D printing, it may reduce formwork stability. The review explores how SCM type, water-to-cement ratio, and superplasticizer dosage affect flowability. It uniquely links rheological properties to practical engineering demands, aiding in the development of high-performance, sustainable cement systems.

Keywords: Clay-based cement; rheology; rheological models; ordinary Portland cement

1. Introduction

In the pursuit of sustainable and low-carbon construction materials, clay-based cementitious systems have gained attention as an alternative to ordinary Portland cement (OPC). Blending limestone and calcined clay has emerged as a promising blend capable of reducing clinker content by up to 50% without compromising mechanical properties [1,2]. One of the challenges in adopting these systems lies in understanding and optimizing their rheological behavior.

Rheology governs the flow, workability, and pumpability of cement pastes, mortars and concrete and is significantly influenced by the physicochemical properties of clay minerals, water to cement (w/c) ratio and the type and dosage of the admixture [3]. Clay minerals vary in particle morphology, surface area, and swelling behavior which affect their interaction with water and other binder components. Unlike OPC paste, which generally exhibits predictable flow behavior, clay-based cement systems demonstrate complex, time-dependent rheology characterized by high thixotropy, increased yield stress (YS), and nonlinear shear response.

Recent studies have provided valuable insights into how factors like NMK, limestone, fly ash (FA), and admixtures influence factors like YS, viscosity, and thixotropy. For instance, limestone calcined clay cement (LC^3) paste requires a superplasticizer (SP) dosage unlike OPC to achieve comparable workability due to strong adsorption by the reactive clay surface. The interaction between water content and solid dispersion dictates whether the mixture behaves in a shear-thinning or shear-thickening manner. Despite the growing interest in rheological behavior in blended systems remains insufficiently understood, especially under varying shear regimes. To fully understand the rheological properties of clay-based cement, a variety of measurement techniques are utilized. Advanced techniques like the use of rheometers are utilized to obtain accurate and precise measurements for rheological properties.

Rheological models play a critical role in characterizing the flow behavior of cementitious materials, providing quantitative parameters such as YS, plastic viscosity, and shear-dependence that are essential for understanding workability, pumpability, and printability. The most widely adopted model in cement rheology is the Bingham model, which assumes a linear relationship between shear stress and shear rate beyond a yield point. While this model performs well for OPC systems, it often falls short in capturing the complex, non-linear rheological behavior exhibited by systems containing supplementary cementitious materials (SCMs). These materials introduce additional interactions such as enhanced flocculation, particle bridging, and rate-sensitive structure breakdown and rebuilding. As such, non-linear models, notably the

*Corresponding author. Email: claremasolia@gmail.com

Appendix B: Sample site for clay A

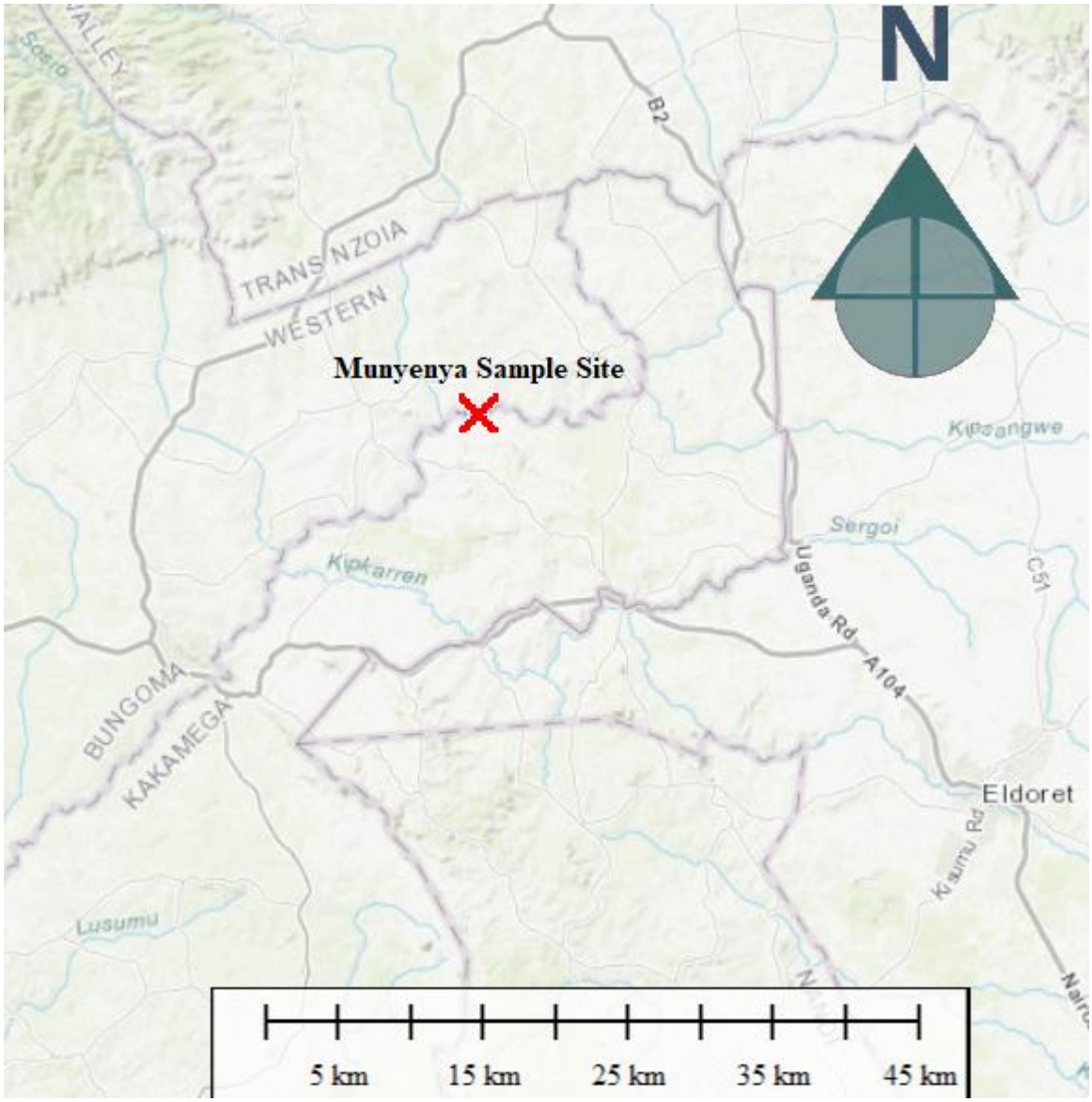

Appendix C: Sample site for clay B

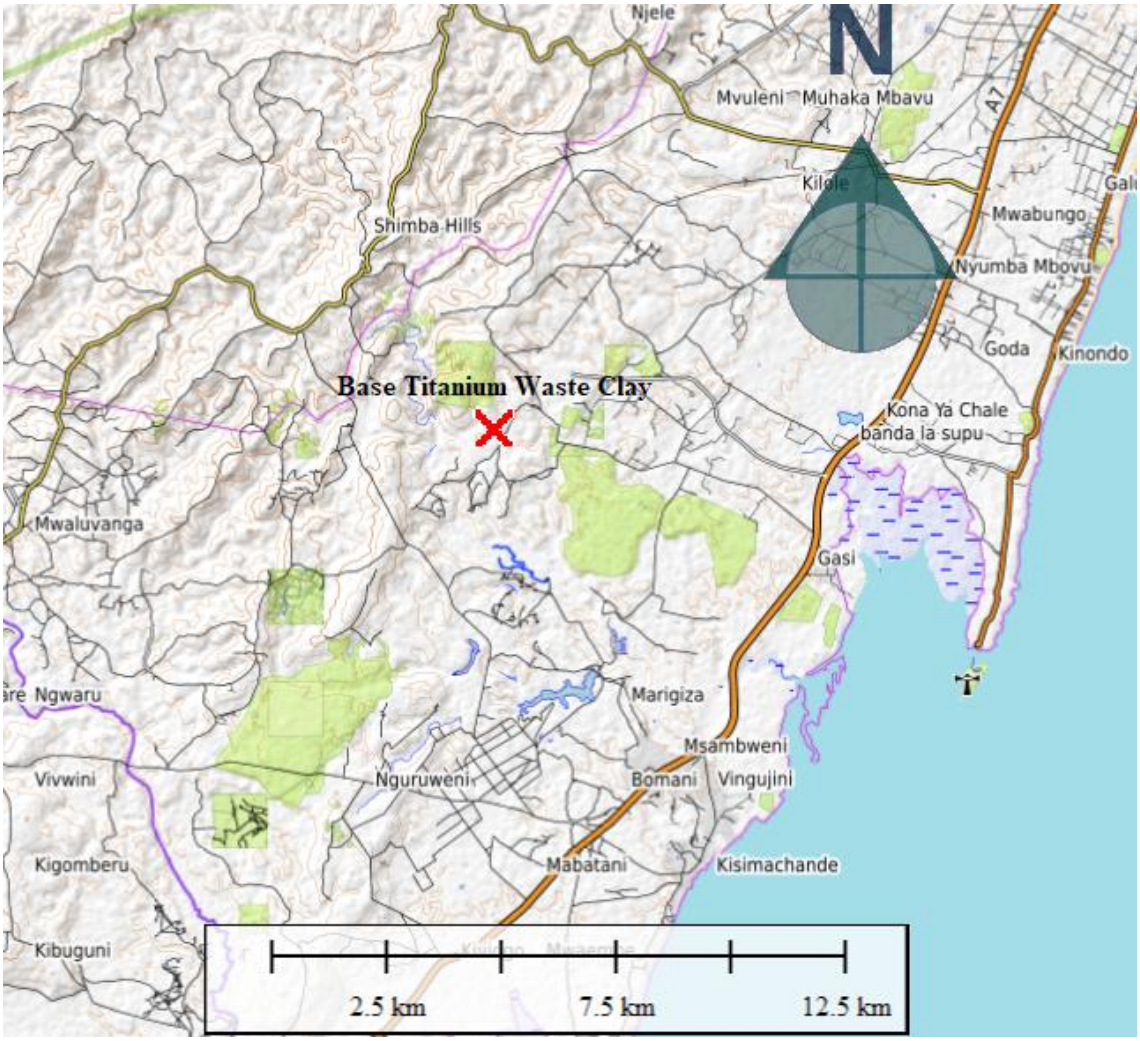

Appendix D: Identified dolomite localities in Kenya

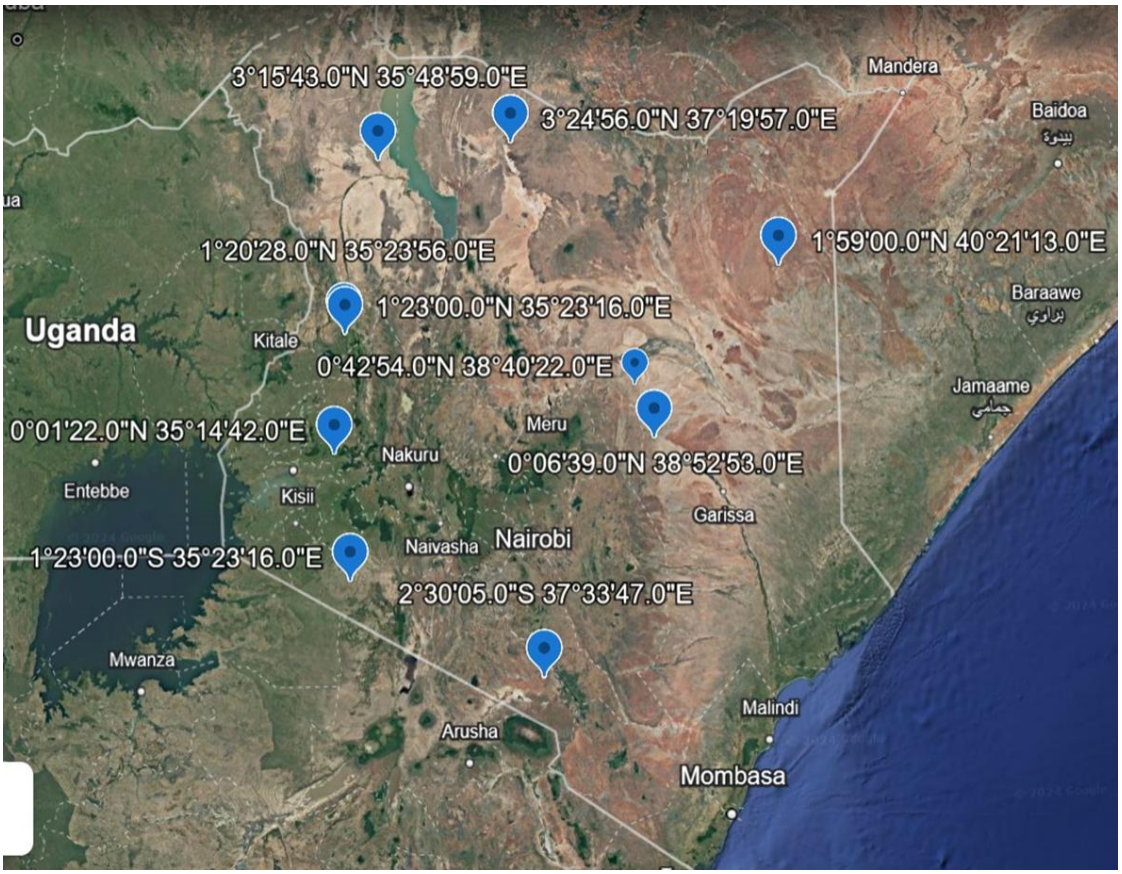

Appendix E: Plagiarism report

DrillBit

The Report is Generated by DrillBit Plagiarism Detection Software

Submission Information

Author Name	CLEAH MINAYO MASOLIA
Title	EFFECT OF DOLOMITE ON STRENGTH, RHEOLOGY AND MICROSTRUCTURE OF TERNARY BLENDED CEMENT
Paper/Submission ID	4259308
Submitted by	mmusungu@must.ac.ke
Submission Date	2025-08-20 15:42:21
Total Pages, Total Words	103, 20749
Document type	Thesis

Result Information

Similarity **12 %**

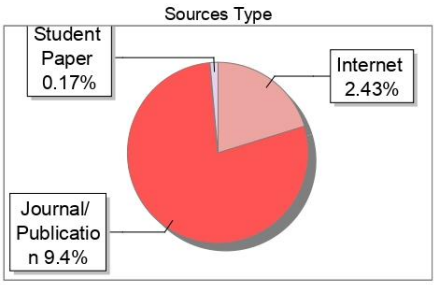

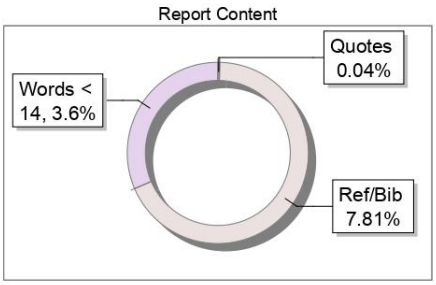

Exclude Information

Quotes	Not Excluded
References/Bibliography	Excluded
Source: Excluded < 14 Words	Not Excluded
Excluded Source	**1 %**
Excluded Phrases	Not Excluded

Database Selection

Language	English
Student Papers	Yes
Journals & publishers	Yes
Internet or Web	Yes
Institution Repository	Yes

A Unique QR Code use to View/Download/Share Pdf File